博士論文番号: 1481201
(Doctoral Student Number)

Induction of oxidative DNA damage by hydroxyurea in *Escherichia coli*

(大腸菌におけるヒドロキシウレアによる DNA 損傷の誘導)

Chang Phooi Yee

Nara Institute of Science and Technology
Graduate School of Biological Sciences
Laboratory of Microbial Molecular Genetics
(Professor Dr. Hisaji Maki)

Submitted on 2018/09/10

Graduate School of Biological Sciences Doctoral Thesis Abstract

Lab name (Supervisor)	Microbial Molecular Genetics (Prof. Dr. Hisaji Maki)		
Name (surname) (given name)	Chang Phooi Yee	Date	2018/09/10
Title	Induction of oxidative DNA damage by hydroxyurea in *Escherichia coli*		

Abstract

The major DNA damage occurs in aerobically growing cells is oxidative DNA damage, caused by the reactive oxygen species (ROS). ROS such as superoxide (O_2^-), hydrogen peroxide (H_2O_2), and hydroxyl radicals (OH•) are produced as by-products of respiration. ROS, especially hydroxyl radicals, attack DNA directly to form various kinds of oxidative DNA damage that leads to genetic instability and cell death. 8-oxoguanine (8-oxoG), a major oxidative DNA damage in normally growing cells, is able to pair equally with cytosine and adenine, resulting in G:C to T:A transversion. In *E. coli*, MutM and MutY are repair enzymes involved in protecting the cell from the mutagenic effects of 8-oxoG. Thus, the mutation assay with strains carrying Δ*mutM* Δ*mutY* double deletions is a powerful tool to determine the oxidative DNA damage level in cells.

Recently, ROS production has been shown to be a consequence of DNA replication stress (DRS). DNA replication process often encounters various endogenous and exogenous obstacles, such as dNTP depletion, inhibition of replication machinery, and blockage of DNA polymerase progression by DNA damages, DNA strand breaks, or DNA unwinding failure. These obstacles would cause slowing or stall of replication fork progression during DNA synthesis, a phenomenon known as DRS. Hydroxyurea (HU), a DRS-inducing agent, has been used extensively as a chemotherapeutic drug. The molecular mechanism proposed for HU action is a direct inhibition of ribonucleotide reductase (RNR), leading to dNTP depletion, which eventually interrupts DNA replication. HU treatment of *E. coli* cells has been reported to indirectly induce the formation of superoxide, which subsequently converts to hydrogen peroxide and produces DNA-damaging hydroxyl radicals when the hydrogen peroxide reacts with ferrous ion (Fe^{2+}). Although HU has been used to study replication fork arrest for decades, the exact downstream physiological effects of HU treatment still remain unclear. In this study, I am interested to refine the current model by studying the effects of HU on oxidative DNA damage and cell death in *E. coli* cells.

By measuring mutation frequencies in Δ*mutM* Δ*mutY E. coli* strain, I found that HU treatment significantly increased the oxidative DNA damages in the cells. Furthermore, the addition of a hydroxyl radical scavenger, thiourea, completely suppressed the HU-induced oxidative DNA damage and cell death. These observations suggest that HU treatment causes hydroxyl radical-mediated oxidative DNA damages and cell death. Since a deletion of gene encoding cytochrome oxidase *bd*-I subunit II prevented HU-induced hydroxyl radical formation in *E. coli* cells, cytochrome oxidase *bd*-I has been suggested to be the source of superoxide under HU treatment. I found that the disruption of cytochrome oxidase *bd*-I significantly suppressed the HU-induced oxidative DNA damage. However, the absence of cytochrome oxidase *bd*-I complex did not significantly affect the cellular levels of superoxide and hydrogen peroxide, suggesting that cellular Fe^{2+} level might be affected by the presence of HU in a manner dependent on the cytochrome oxidase *bd*-I complex. Further investigation using plasmids carrying *cydAB* genes either in wild-type or mutated forms shows that *E. coli* cells expressing cytochrome oxidase *bd*-I with reduced heme content suppress the HU-induced oxidative DNA damages and cell death. In contrast, there is no significant reduction in oxidative DNA level in cells expressing functional-defective cytochrome oxidase *bd*-I. These results suggested that the oxidase activity of cytochrome oxidase *bd*-I is not required for HU-induced oxidative DNA damage and cell death. Heme from cytochrome oxidase *bd*-I might play a role in HU-induced oxidative DNA damages and cell death, probably by affecting the intracellular Fe^{2+} level.

To examine whether the induction of oxidative DNA damage by HU treatment can be generalized for other DNA replication arrest condition, I determined the oxidative DNA damage level in *E. coli* strains defective in DNA replication machinery. The oxidative DNA damage level in *E. coli* temperature-sensitive Pol III mutant, *dnaE486*, was significantly increased when the cells were transferred to non-permissive temperature. This increased oxidative DNA damage in *dnaE486* cells can be suppressed by the addition of thiourea or partially suppressed by iron chelator bipyridine. These results suggested that DNA replication arrest induced by inactivation of replication machinery leads to oxidative DNA damages in cells via hydroxyl radical formation. However, disruption of cytochrome oxidase *bd*-I did not suppress the induction of oxidative DNA damages in the *dnaE486* mutant, suggesting that the mechanisms of oxidative DNA induction are different between the HU-treated cell and Pol III mutant.

In summary, this study highlighted the mechanism of HU-induced oxidative DNA damage, whereby HU induces the generation of hydroxyl radical, which cause oxidative DNA damages and cell death. The production of hydroxyl radical in HU-treated cells is likely due to the damage of cytochrome oxidase *bd*-I that may release heme from the protein and probably affect the intracellular free Fe^{2+} level. This study further expanded our understanding of the effects of HU treatment, which could help to improve the current cancer treatment.

Abbreviations

8-oxoG	8-oxoguanine
BER	Base excision repair
dNTP	Deoxyribonucleotide triphosphate
DRS	DNA replication stress
DSB(s)	DNA double strand break(s)
EDF	Extracellular death factor
GFP	Green fluorescent protein
HR	Homologous recombination
HU	Hydroxyurea
NHEJ	Non-homologous end joining
RNR	Ribonuleotide reductase
ROS	Reactive oxygen species
SOD	Superoxide dismutase
ssDNA	Single-stranded DNA
WT	Wild-type

List of contents

List of figures

List of tables

Chapter 1 Introduction

1. Reactive oxygen species and oxidative DNA damages

Oxidative damage is an inevitable biological problem in aerobic organisms. It usually has devastating effect on DNA, RNA, membrane and proteins, resulting in mutagenesis, aging or cell death. Oxidative damage is caused by reactive oxygen species (ROS), including superoxide (O_2^-), hydrogen peroxide (H_2O_2), and hydroxyl radical (OH•). In bacteria growing in an aerobic environment, oxygen crosses the membrane freely and react with univalent electron donors, such as metal centers, dihydroflavin cofactors ($FADH_2$ cofactors), and quinones to form ROS. The overall reaction rate is directly depending on the concentration of intracellular oxygen. In *E.coli*, the formation of H_2O_2 is approximately 15 μM/sec in well-fed cells, whereas superoxide production estimated to be about 5 μM/sec (Imlay, 2008).

The respiratory chain is the main source of superoxide. During the respiration process, superoxide is released from the external face of the cytoplasmic membrane to the periplasm (Korshunov & Imlay, 2006). Superoxide is less stable compared to H_2O_2 and it is quickly converted to H_2O_2 by superoxide dismutase (SOD). When H_2O_2 comes into contact with the cellular unincorporated ferrous ion (Fe^{2+}), hydroxyl radical can be formed through Fenton reaction:

$$Fe^{2+} + H_2O_2 \rightarrow Fe^{3+} + OH\bullet + OH^-$$

Hydroxyl radical is the most reactive and the least stable form of oxygen. It can oxidize and destroy many cell components such as nucleic acids, lipids and proteins. Oxidative DNA damage is the most abundant, with a high rate of approximately 10^5 lesions per human cell per day (Bridge et al., 2014). Hydroxyl radical reacts with purine bases, pyrimidine bases and sugar moiety of the DNA backbone to produce various kinds of oxidative DNA damages (Dizdaroglu, 2012). The majority of the oxidized pyrimidine found in the cells are thymine glycol and cytosine glycol. Thymine glycol is the DNA lesion that blocks DNA replication, whereas cytosine glycol is an unstable lesion that quickly hydrates or deaminates to form 5-hydroxycytosine (5-OHC) or 5-hydroxyuracil (5-OHU), resulting in GC to AT transition mutations (Kreutzer & Essigmann, 1998; Kung & Bolton, 1997). On the other hand, the most commonly oxidized purine by hydroxyl radical is 7,8-dihydro-8-oxoguanine (8-oxoG). Due to the low redox potential, 8-oxoG became the major form of oxidative DNA damages in the cells (Neeley & Essigmann, 2006). 8-oxoG is able to pair with cytosine (C) and adenine (A) equally during DNA synthesis (Maki & Sekiguchi, 1992). Misincorporation of adenine opposite to 8-oxoG can lead to G:C to T:A transversions when unrepaired.

1.1 Scavenging systems against superoxide and hydrogen peroxide in *E. coli*

As shown in **Figure 1.1**, both superoxide and H_2O_2 can lead to the production of hydroxyl radical and, thus, are potentially mutagenic to the cells. In order to maintain low intracellular concentration of ROS, bacteria commonly synthesize scavengers as their front-line defense against the excess superoxide and H_2O_2.

SOD is an antioxidant that catalyzes the dimutation of superoxide into either oxygen or H_2O_2 by adding or removing an electron. SOD restricts the intracellular superoxide level to approximately 0.1 nM (Imlay, 2008). *E.coli* contains two cytoplasmic SOD (MnSOD and FeSOD) and a periplasmic SOD (CuZnSOD) (Alhama et al., 1998). The genes for MnSOD, FeSOD and CuZnSOD are designated as *sodA*, *sodB* and *sodC* respectively. Mutants defective in both MnSOD and FeSOD are not SOD null because they still contain ~2% of the periplasmic CuZnSOD, which is expressed during the late stationary phase (Benov & Fridovich, 1994). Because superoxide cannot easily cross the cell membrane, *E.coli* requires different SOD to maintain superoxide level in the cytoplasm and periplasm separately.

The primary endogenous H_2O_2 scavenger in *E. coli* is the OxyR-regulated peroxiredoxin AhpCF, which is a two-component NADH peroxidase. Ahp catalyzes the reduction of H_2O_2 to water. The activity of Ahp is so high that it maintains the steady-state concentration of H_2O_2 at less than 20 nM (Seaver & Imlay, 2001b). However, when the intracellular concentration of H_2O_2 exceeds 20 nM, Ahp becomes saturated. In this case, OxyR-regulated catalase (catalase G) is strongly induced and became the predominant scavenger against H_2O_2 in the cells (Seaver & Imlay, 2001a).

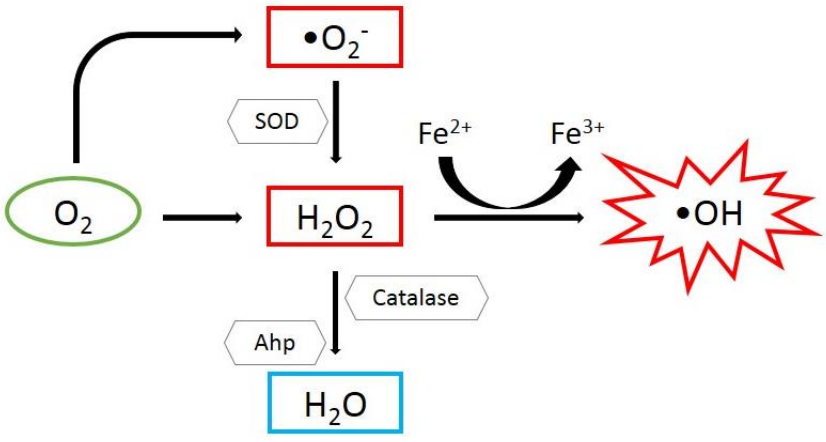

Figure 1.1 Formation of OH• and ROS scavenging systems in *E. coli*.

1.2 Control of intracellular unincorporated iron

Iron is essential for most organisms. It participates in many major biological processes such as gene regulation, respiration, tricarboxylic acid (TCA) cycle, and oxygen transport. However, hydroxyl radical is formed by the reaction between H_2O_2 and ferrous iron (Fe^{2+}) (**Figure 1.1**), thus iron regulation is important to limit the production of hydroxyl radical in cells.

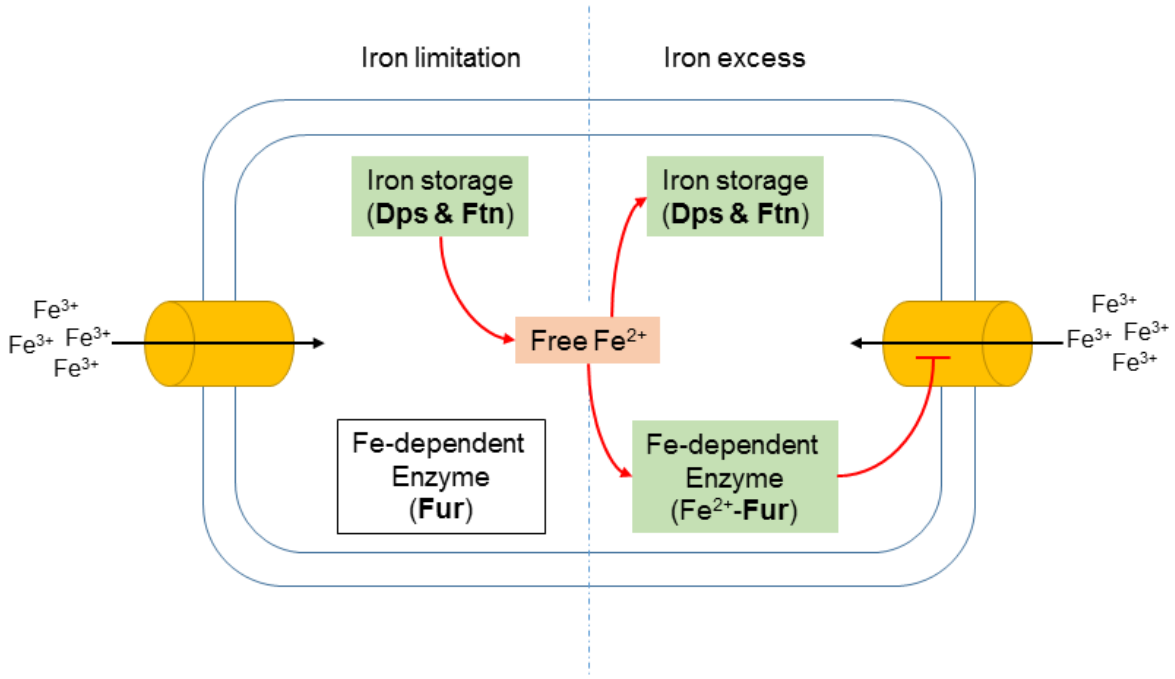

Figure 1.2 Mechanism of cellular iron regulation in *E. coli* cells.

The iron content of *E. coli* is ranging from ~ 10^5-10^6 atoms per cell depending on the growth conditions (Andrews et al., 2003). *E.coli* contains ferric uptake regulator (Fur), ferritin (Ftn) and DNA-binding proteins from starved cells (Dps) to regulate the intracellular ferrous iron concentration (**Figure 1.2**). Fur protein is a transcription factor which can be activated by binding of ferrous iron. Activated Fur represses the operons that encode iron transportation proteins such as TonB, ExbB and ExbD. When *fur* gene is mutated, the unincorporated iron level rose to five- to ten-fold and the cells exhibited high mutagenesis rate (Keyer & Imlay, 1996; Touati et al., 1995).

FtnA and Dps belong to the iron-storage proteins, which regulate the intracellular ferrous iron. FtnA is one of the major non-haem iron storage proteins found in animals, plants, and microorganisms. Dps is the iron-storage protein found only in bacteria. FtnA is the major iron-storage protein in *E. coli* responsible for the ≤ 50% of the total cellular iron during iron-

sufficient conditions and provides a source of iron during iron-deficient conditions (Abdul-Tehrani et al., 1999). As a ferritin-like protein, Dps has been reported to protect *E. coli* from oxidative DNA damage via its DNA-binding activity and ferroxidase activity (Karas et al., 2015). During stationary phase, Dps binds to the chromosome non-specifically to form a stable Dps-DNA co-crystal, protecting the DNA from oxidative damage. The lysine residues found in the N-terminal region of Dps are the source of positive charge that allow DNA binding to occur (Calhoun & Kwon, 2011). Because of its ability to carry out ferroxidase activity, Dps family members contain a highly conserved ferroxidase center where oxidation of Fe^{2+} ions took place. The resulting Fe^{3+} ions are stored within the Dps cavity.

Recently, Mironov's group discovered a new defensive pathway against oxidative stress in *E. coli*, which is endogenous hydrogen sulfide (H_2S)-mediated iron regulation (Mironov et al., 2017). Their findings revealed that 3-mecaptopyruvate sulfurtransferase (3MST), which is the major source of endogenous H_2S in *E. coli*, protects the cells against oxidative stress via L-cysteine utilization and H_2S-mediated sequestration of ferrous iron.

1.3 Action of MutM, MutY and MutT in oxidative DNA damage repair

In normally growing cells, ROS is maintained at low levels by the effective action of antioxidants. However, when the balance between ROS and antioxidants is interrupted, the cellular level of ROS could be increased and induce oxidative stress. One of the deleterious outcomes of oxidative stress is the production of 8-oxoguanine (8-oxoG). 8-oxoG is capable of pairing equally effectively with both adenine (A) and cytosine (C) during DNA synthesis (Maki & Sekiguchi, 1992). 8-oxoG is a highly mutagenic base analog either in the form of 8-oxoG in DNA or 8-oxodGTP. To combat the mutagenic consequences of 8-oxoG, organisms have developed cellular defense mechanisms. Among the repair pathways, the base excision repair (BER) pathway is the most important cellular protection mechanism responding to oxidative DNA damage. In *E. coli*, BER glycosylases such as MutM and MutY, and an 8-oxo-dGTP diphosphatase MutT, protect the cells from the mutagenic effects of oxidative guanine (Fowler et al., 2003; Tajiri et al., 1995).

MutM and MutY are glycosylases which repair the misincorporation of nucleotides due to the formation of 8-oxoG in DNA. MutM (formamidopyrimidine-DNA glycosylase/ Fpg protein) acts upon 8-oxoG and initiates BER against 8-oxoG that paired with C. MutY is an adenine glycosylase active on DNA containing A:8-oxoG, A:G, and A:C mismatches (Michaels et al., 1992) but it has a weak guanine glycosylase activity (Li et al., 2000). MutY is responsible for removing misincorporated adenines paired with 8-oxoG and reduces the 8-oxoG mutational effects. Deficiencies in *mutM* or *mutY* result in high G:C to T:A transversion rate. However, the

mutM mutY double mutator strain has a G:C to T:A transversion rate 20-fold higher than the sum of the single mutation rate (Michaels et al., 1992). This indicated that MutM and MutY protect cells from the mutational effects of 8-oxoG through different steps in the same pathway.

On the other hand, MutT protein controls the 8-oxodGTP level in the dNTP pool by hydrolyzing 8-oxodGTP into 8-oxodGMP and pyrophosphate, reducing the chance of 8-oxodGTP being used as a substrate by DNA Polymerase III during DNA synthesis. Maki and Sekiguchi showed that MutT hydrolyzes 8-oxodGTP 10 times faster than dGTP and concluded that 8-oxod-GTP is the biological substrate for MutT (Maki & Sekiguchi, 1992). Defective mutant of *mutT* shows up to 100-10,000-fold enhancement of A:T to C:G transversions without any effect on other types of mutations (Fowler & Schaaper, 1997).

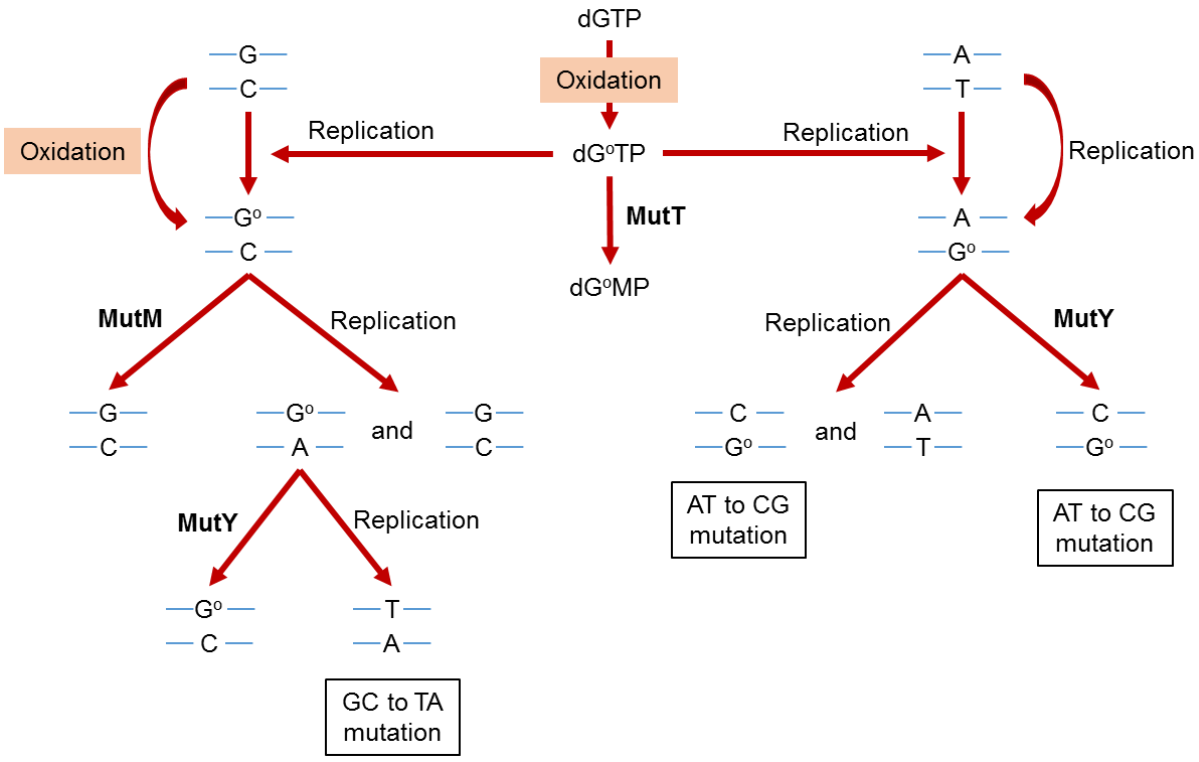

Figure 1.3 Oxidative DNA damage repair mechanism mediated by MutM, MutY and MutT.

2. DNA replication stress

In normal condition, the average speed of replication fork in *E. coli* is ~900 nt/sec (Kim *et al.*, 1996; Pham *et al.*, 2013). In human, the replication fork moves at a rate of 50 nucleotides per second, approximately 20 times slower than the prokaryotic cells (Alberts et al., 2002). However, replication fork progression is often encountered various endogenous or exogenous obstacles that can lead to replication fork stalling. Replication fork will become slow or come to a stop when encountering obstacles such as DNA damages or fork barriers (eg. secondary DNA structure) (Bierne & Michel, 1994). Besides that, malfunction of replication machinery and dNTP depletion also lead to replication fork stalling (Belle et al., 2007; Bester et al., 2011; Poli et al., 2012; Wechsler & Gross, 1971). These obstacles would cause slowing or stall of replication fork progression during DNA synthesis, a phenomenon known as DNA replication stress (DRS). DNA replication stress is one of the factors that cause genome instability and cell death in both prokaryotic and eukaryotic cells. DNA replication stress or replication fork arrest usually causes an increase in single-stranded DNA (ssDNA) which act as the signal to activate the cell cycle checkpoints (Sabatinos & Forsburg, 2015). The accumulation of ssDNA can further lead to DNA double strand breaks (DSBs) (Feng et al., 2011). DNA double strand breaks are lethal to the cells, and it needs to be repaired in order for the DNA replication to resume. To ensure faithful and complete DNA replication, cells coordinate specific pathways such as the homologous recombination (HR) to repair the DNA double strand breaks and to facilitate fork restart (Bierne & Michel, 1994; Carr & Lambert, 2013).

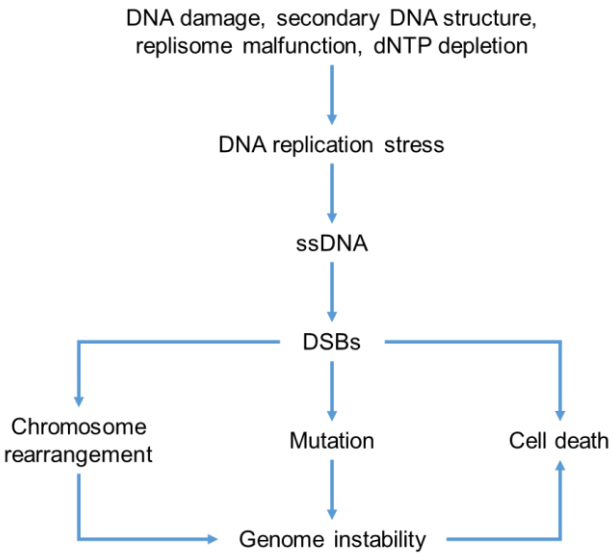

Figure 1.4 Sources and consequences of DNA replication stress.

2.1 Sources of DNA replication stress

2.1.1 Exogenous sources

Any agents that inhibit or block replication fork progression can cause DNA replication stress. UV-light is an example of physical agent that can cause replication stalling in the cells. UV-light is capable of ionizing molecules through a process called photochemical reaction that leads to the formation of new molecular products. The most common photochemical product in DNA is the cyclobutane pyrimidine dimer. This product is formed when two adjacent pyrimidines (thymines, TT, or cytosines, CC) linked covalently by their C=C double bonds (Sinha & Häder, 2002). These four carbons form a cyclic ring (cyclobutane) that links the two pyrimidines, thus creating a chemical intermediate in the DNA. This photochemical product alters the DNA structure, consequently inhibiting DNA synthesis by replicative DNA polymerases and leading to replication arrest. Formation of pyrimidine dimers is the primary cause of skin cancers in human (Soehnge et al., 1997).

Chemicals that are commonly used in anti-cancer chemotherapy can cause replication arrest by forming the intra-strand and inter-strand crosslinks, DNA-protein crosslinks, double-strand DNA breaks and DNA base damages. Typical crosslinking agents introduce covalent bonds to the nucleotides located on the same strand (intrastrand crosslinks), like cisplatin, or opposite strands (interstrand crosslink), like mitomycin C (Dasari & Tchounwou, 2014; Weng et al., 2010). Crosslinks block the replication fork progression by inhibiting the DNA strands unwinding and separating process. Hydroxyurea (HU) is an anti-cancer drug that reduces the dNTP pool by inhibiting ribonucleotide reductase (RNR), which is involved in the dNTP biosynthesis, subsequently slowing down or arresting DNA replication fork progression (Poli et al., 2012). Both Camptothecin and etoposide which are the inhibitors of topoisomerase I and topoisomerase II, respectively, block replication fork progression by preventing the DNA unwinding and religation process after topoisomerase-mediated cleavage (Liu et al., 2006; Montecucco et al., 2015).

2.1.1.1 Hydroxyurea (HU)

Hydroxyurea (HU) was first synthesized in 19th century. It inhibits the biosynthesis of dNTP by interfering the class Ia ribonucleotides reductase (RNR) enzyme. Class I RNR is a large tetrameric enzyme comprising of two R1 subunits and two small regulatory subunits R2. RNR catalyzes the conversion of ribonucleotides to deoxyribonucleotides under aerobic condition (Kolberg et al., 2004). HU inhibits the RNR enzymatic activity by scavenging the tyrosyl free radical of the R2 subunit, leading to dNTP pool depletion and subsequently prevent DNA replication in both prokaryote and eukaryote cells.

HU was first approved as the medicine for the treatment of neoplastic disorders in the 1960s, followed by the treatment of sickle cell disease in 1998 (Segal et al., 2008). HU was also used for the treatment of essential thrombocytosis and polycythemia vera (Barbui et al., 2012), as well as myeloproliferative disorders and psoriasis (Lee et al., 2011; Segal et al., 2008). Besides that, HU was also used extensively in research for cell cycle synchronization, DRS induction, and checkpoint responses (Barthelemy et al., 2016; Darzynkiewicz et al., 2011; Morafraile et al., 2015).

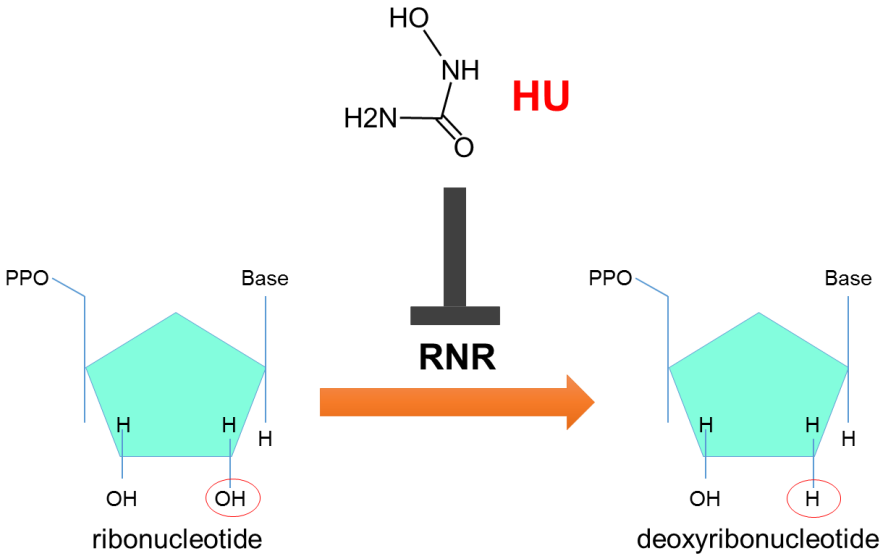

Figure 1.5 Hydroxyurea (HU) reduces the dNTP pools by inhibiting the ribonucleotide reductase (RNR).

2.1.2 Endogenous sources

Several endogenous sources constantly challenge the DNA replication progression and cause replication fork arrest. These endogenous sources include unrepaired DNA lesion, unusual DNA structure, and limitation of essential replication factors.

Unrepaired DNA lesion is one of the most commonly recognized sources of DNA replication stress. DNA lesions are formed by the action of intrinsic factors such as errors generated during DNA replication and oxidative damage by reactive oxygen species (ROS) produced from respiratory chain. Besides that, unusual secondary DNA structure formation can also lead to DRS. Inverted repeats of DNA are capable of forming unusual hairpin structure, which block replication fork progression (Voineagu et al., 2008).

DNA replication requires a number of components that can slow replication fork speed and induce DNA replication stress when they are being limited. These factors include

nucleotides availability and the replication machinery such as DNA polymerase and DNA helicase (Belle et al., 2007; Bester et al., 2011; Poli et al., 2012; Wechsler & Gross, 1971). In addition, improper control of replication initiation can also be a source of DNA replication stress, as firing too many origins at one time can deplete nucleotide pool and slow down the replication fork speed (Beck et al., 2012; Sørensen & Syljuåsen, 2012).

2.2 Consequences of DNA replication stress

One of the earliest consequences of DNA replication stress is the formation of single-stranded DNA (ssDNA). Stretches of ssDNA are often found at the stalled replication forks as the consequence of replicative helicases continuing to unwind the parental DNA even after the replicative DNA polymerase has stalled (Mazouzi et al., 2014; Zeman & Cimprich, 2014). Replication arrest-induced ssDNA activates the SOS response in bacteria or ATM- and Rad3-related (ATR) kinase in eukaryotic cells, to ensure that the stalled fork is able to restart (Davies et al., 2009; Flynn & Zou, 2011; Walker, 1984). However, prolonged exposure of DNA replication stress can lead to DNA double-strand breaks (DSBs), which is caused by the accumulation of ssDNA at the stalled forks. DSBs are lethal to the cells, and it needs to be repaired to preserve chromosomal integrity. DSBs are repaired predominantly by non-homologous end joining (NHEJ) and homologous recombination (HR). HR is the exclusive mechanism for DSB repair in *E. coli* (Motamedi et al., 1999). When an excess number of unrepaired DSBs accumulate in the DNA, cells will commit suicide by activating the cellular death program, a process known as programmed cell death.

Defects in cellular responses to DNA replication stress are always associated with human genetic diseases and cancer predisposition (Mazouzi et al., 2014; Muñoz & Méndez, 2017). Meier-Gorlin Syndrome is a disease whereby patients display severe growth retardation and developmental malformations. Meier-Gorlin Syndrome is linked to the mutations in the pre-replication factors ORC1, ORC4, ORC6, Cdc6 and Cdt1. Other examples of DNA replication stress-related syndromes such as Bloom, Rothmud-Thomson and Werner, in which mutations affect the DNA helicase BLM, RECQL4 and WRN, respectively. The patients suffering from these syndromes have some common characteristics such as growth defects and premature aging. Besides the genetic conditions, DNA replication stress also contributes to cancer predisposition. The cancer-prone human syndromes related to DNA replication stress include Ataxia telangiectasia, Nijmegen breakage syndrome, hereditary breast and ovarian cancer syndrome, Fanconi anaemia, Bloom syndrome, Rothmud-Thomson syndrome and Werner syndrome (Gaillard et al., 2015).

3. Objectives of this study

DNA replication stress refers to the phenomenon when DNA replication fork progression is being slowed down or arrested by endogenous or exogenous obstacles. DNA replication stress is believed to be one of the factors that cause genome instability and cell death. In DNA replication stress condition, single-stranded DNA (ssDNA) and DNA double strand breaks (DSBs) are found at the stalled fork. Various cellular repair systems and checkpoint machinery are activated to repair the DNA damages and facilitate the restart of the stalled fork. However, when a number of unrepaired DNA damage accumulates, the cell will commit suicide by activating the cellular death program.

Hydroxyurea (HU) is an anti-cancer drug, which is also used extensively in the laboratory to inhibit DNA replication and cell division. HU induces DNA replication stress by inhibiting the class I ribonucleotide reductase (RNR) enzyme and effectively depleting the dNTP pools in the cells. Recently, Davies *et al.* proposed that HU treatment induces the production of superoxide, which subsequently leads to cell death via hydroxyl radical formation (**Figure 1.6**). They proposed that the MazEF toxin-antitoxin, the Cpx membrane stress response system, and the cytochrome oxidase *bd*-I are involved in the HU-induced cell death. They believed that the MazF toxin is activated upon HU treatment and the activated MazF cleaves mRNAs, leading to incomplete protein translation. Misfolding of proteins then triggers Cpx membrane stress response, which upregulates the genes responsible for protein folding and degradation. All these effects alter the properties of cytochrome oxidase *bd*-I, causing an increase in superoxide production. The increased superoxide production accelerates the formation of hydroxyl radical in the cells, which lead to cell death. However, their model contains several unclear speculations. There is no direct evidence to show that the activation of the MazF toxin is due to the DNA replication arrest upon HU treatment. Furthermore, there is also no direct evidence to prove the involvement of cytochrome oxidase *bd*-I in superoxide production in their study. If the proposed model by Davies *et al.* is correct, this will raise the question whether hydroxyl radical caused cell death in the HU-treated cells through oxidative DNA damage. Since hydroxyl radical has a short lifespan, the use of hydroxyphenyl fluorescein (HPF) to determine the hydroxyl radical level in their study raised another question of whether their data reflect the actual intracellular hydroxyl radical level.

Although HU has been used to study replication fork arrest for decades, the exact physiological effects of HU treatment remain unclear. In this study, I am interested to refine the current model by studying the effects of HU on oxidative DNA damage and cell death in *E. coli* cells.

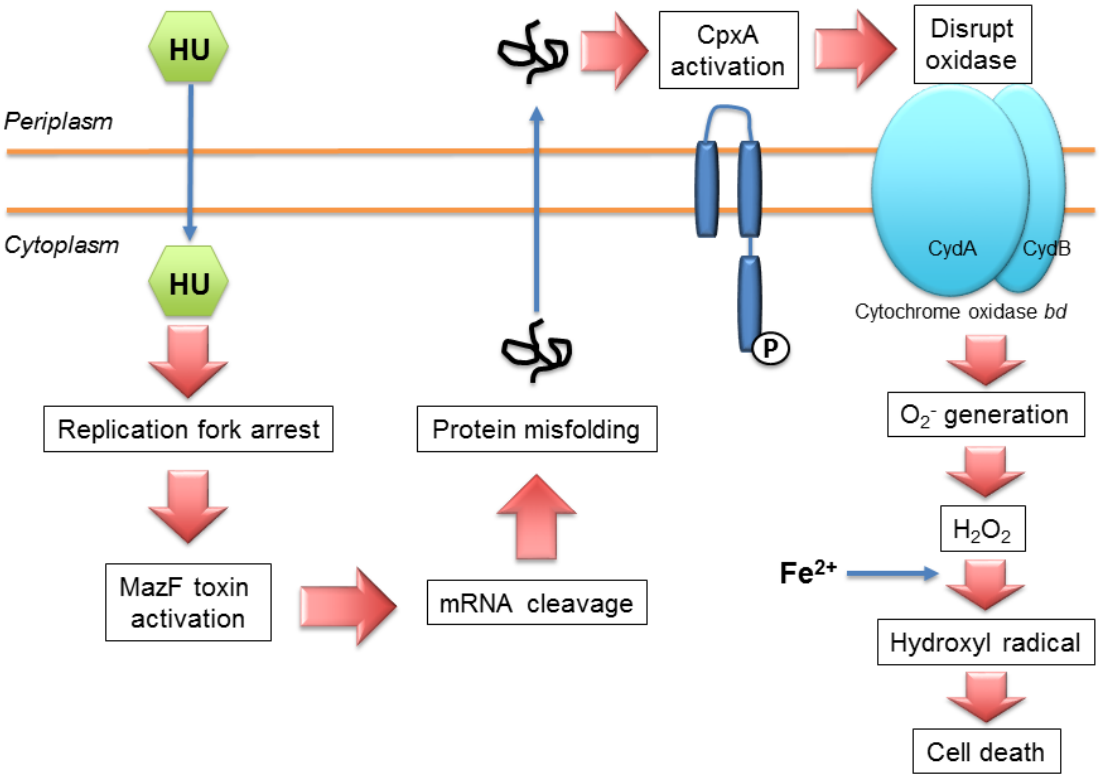

Figure 1.6 Schematic model of HU-induced cell death in *E. coli* cell proposed by Davies *et al.*, 2009.

Chapter 2 Materials and Methods

1. Materials

1.1. Bacterial strains and plasmids

All *E. coli* strains used in this study are listed in Table 2.1. Single-gene deletion mutants were obtained from *E. coli* KEIO Collection (NBRP) and used to construct double, triple, and quadruple mutants by P1 transduction. Details of strain construction are described in section 2.1. All mutants used in the experiments are MG1655 background. Δ*mutM* Δ*mutY* double-mutant was used as wild-type (WT) unless otherwise stated. Plasmids used in this study are listed in Table 2.2.

Table 2.1 Strains used in this study

Strain name	Genotype	Source
MG1655	F-, λ-, *rph-1*	(Guyer et al., 1981)
BW25113	*rrnB3* Δ*lacZ4787 hsdR514* Δ*(araBAD)567* Δ*(rhaBAD)568 rph-1*	(Datsenko & Wanner, 2000)
JW3882	BW25113 Δ*cpxA*::kan	Keio collection
JW2753	BW25113 Δ*mazF*::kan	Keio collection
MK7180	MG1655 Δ*mutM* Δ*mutY*	Laboratory stock
MK10103	MK7180 Δ*cpxA*::kan	This study
MK10104	MK7180 Δ*cpxA*	This study
MK9313	MK7180 Δ*cydAB*	Laboratory stock
MK9310	MK7180 Δ*cyoABCD*	Laboratory stock
MK9312	MK7180 Δ*cbdAB*	Laboratory stock
MK10101	MK7180 Δ*mazF*::kan	This study
MK10102	MK7180 Δ*mazF*	This study
MK7127	MG1655 *dnaE486*(Ts),Tn10	Laboratory stock
MK10107	MK7180 *dnaE486*(Ts),Tn10	This study
MK10109	MK10107 Δ*cpxA*	This study
MK10110	MK10107 Δ*cydAB*	This study
MK10108	MK10107 Δ*mazF*	This study
MK6313	MG1655 *dnaB42*(Ts)	Laboratory stock
MK10111	MK6313 malF3089::Tn10	This study
MK10112	MK7180 *dnaB42*(Ts), Tn10	This study

Table 2.2 Plasmids used in this study

Plasmid name	Genotype	Source
pCP20	FLP, *amp*^{r}, *cm*^{r}	(Datsenko & Wanner, 2000)
pTN247	pSTV29, *soxS*-GFP	(Nakayashiki & Mori, 2013)
pTN249	pSTV29, *ahpC*-GFP	(Nakayashiki & Mori, 2013)

1.2 Synthetic oligonucleotides

Synthetic oligonucleotides were obtained from Integrated DNA Technologies and purified by HPLC. The oligonucleotide after purification was stored in TE buffer (10 mM Tris-HCl (pH8.0), 1 mM EDTA) and store at -20˚C.

Table 2.3 Oligonucleotides used in this study

Name	Sequence (5'-3')	Purpose
SA1	ATCCAGTGTTCGCCAGCACGT	Screen for Δ*mutM*
SA2	CATCAGGCGCTGATGGCGAAG	
SA3	GTTGCCGGATGCAAGCATGATAAG	Screen for Δ*mutY*
SA4	CTGACCTTCTGCTTCACGTTGC	
cpxA-F	CCGGTTGTGGGGAAAATAAC	Screen for Δ*cpxA*
cpxA-R	GACACTGGAAGTTGATGCCTTAG	
cCYD-F	AAAGAATTAAGGTCAACCG	Screen for Δ*cydAB*
cCYD-R	CGCCCGCAGGGGGCGCTTGTCCAT	
cCYO-F	ATAACGCCCTTTTGCAACAG	Screen for Δ*cyoABCD*
cCYO-R	GTTAAACACACAACCCGACGCCACA	
cCBD-F	GCTTAGCGAGGTATGTCAGT	Screen for Δ*cbdAB*
cCBD-R	ATGTTTCCGCTTTTCATATCTGACA	
mazF-F	GGCGCTGCATAATAGTGAGCAAAC	Screen for Δ*mazF*
mazF-R	CTGAACTGGTCAACGACATCACG	

dnaE486-F dnaE486-R	CGAAATCGTGTATGGTATTGGC ATACTGGTTGATAGGGTGTCC	Sequencing of *dnaE*
cydABXE-EcoRI-F	GCCGAATTCATTTTGCGTTTAT CTTCAC	Construction of *cydABXE* on pCYDAB
cydABXE-BamHI-R	GCCGGATCCTTAAAAGAAGAA GAAAATC	
cydAB-E99A-F	GCAATCGCAGGTCTGATGGCCT TCTTC	Site-directed mutagenesis in *cydABXE* on pCYDAB
cydAB-E99A-R	CAGACCTGCGATTGCCAGCGG CGCACC	
cydAB-K252A-F	GAAAACCGCTCTGGCTGCTATT GAAGCC	Site-directed mutagenesis in *cydABXE* on pCYDAB
cydAB-K252A-R	CAGCCAGAGCGGTTTTCTGCAC GTCGCC	

1.3 Chemicals and media

**Chemicals*

For PCR reactions: rTaq DNA polymerase, dNTPs mix and rTaq buffer were supplied from BioAcademia, and PrimeSTAR® Max was supplied from Takara.

For DNA sequencing: BigDye™ Terminator v3.1 ready reaction mix and BigDye™ Terminator v3.1 5X sequencing buffer were supplied from Thermo Fisher Scientific. 70% ethanol was used for DNA purification and Hi-Di™ Formamide (Thermo Fisher Scientific) was used for sequencing.

For restriction enzyme digestion: *Eco*RI and *Bam*HI were supplied from Toyobo. *Dpn*I was supplied from Takara.

**Media*

LB medium: 1% (w/v) bacto tryptone, 0.5% (w/v) bacto yeast extract, 1% (w/v) NaCl, pH 7.0. LB agar was prepared by adding 1.5% bacto agar into LB. The medium was autoclaved at 121 ˚C for 20 min before use.

R-top soft agar and R plate agar: 1% (w/v) bacto tryptone, 0.1% (w/v) bacto yeast extract, 0.8% (w/v) NaCl, 1.2% (w/v) bacto agar were autoclaved at 121 ˚C for 20 min. After the medium cooled down to 50 ˚C, 2 mM CaCl2 and 0.1% glucose were added. For the R-top soft agar, 0.8% (w/v) bacto agar were used.

Antibiotics: The final concentrations of ampicillin, kanamycin, tetracycline,

chloramphenicol, and rifampicin were used as 100 μg/mL, 50 μg/mL, 10 μg/mL, 25 μg/mL, and 100 μg/mL, respectively. The antibiotic stocks were prepared by dissolving antibiotics in MilliQ water and sterilized by 0.2 μm filter, except for chloramphenicol, rifampicin, and tetracycline. To prepare chloramphenicol and rifampicin stock solutions, rifampicin or chloramphenicol was dissolved in methanol. Tetracycline stock solution was prepared by dissolving tetracycline powder in 70% ethanol.

2. Methods

2.1. Mutant strains construction

2.1.1 Non temperature-sensitive mutants

2.1.1.1 P1 donor lysate preparation

A single colony of donor strains (KEIO strains) was picked and grown in 5 mL LB overnight at 37˚C. Next day, overnight culture was diluted in 5 mL LB supplemented with 5 mM $CaCl_2$ at 1:100 and incubated at 37˚C with shaking until OD_{600} reached 0.4 – 0.5 ($1x10^8$ cells/mL). One mL of an exponentially growing culture was mixed with P1 *vir* lysate ($1x10^7$ pfu/mL). The mixture was incubated at 37˚C for 20 min without shaking. At the end of the incubation, the mixture was transferred and mixed with 2.5 mL warmed R-top soft agar containing 5 mM $CaCl_2$ and 0.2% glucose. The mixture was poured gently and distributed evenly on R-plate. The plate was incubated approximately 8 hrs at 37˚C. When high density of plaques was observed from the plate, the soft agar was collected, and transferred into a centrifuge tube. The surface of agar was washed using 1.5 mL LB and the LB was transferred into the same centrifuge tube. Chloroform (100 μL) was added into the tube and followed by vortex until the soft agar dissolved completely. After centrifugation at 9,000 rpm for 20 min, the supernatant was transferred into a new tube, and 2 drops of chloroform were added. The supernatant (P1 donor lysate) was stored at 4˚C.

2.1.1.2 P1 Transduction

An overnight culture of recipient strain was 1:100 diluted in 5 mL LB and incubated at 37˚C with shaking until OD_{600} reached 0.8-1.0. The culture was spun down at 5,000 rpm for 5 min and resuspend the pellet in 1 mL MC buffer (100 mM $MgSO_4$ and 5 mM $CaCl_2$). The resulting sample contained $1x10^9$ cells/mL. Transduction was done by mixing $1x10^8$ cells/mL of the recipient with $1x10^8$ pfu or $1x10^7$ pfu of donor lysate and incubated at 37˚C for 30 min. Sodium citrate (5 mM) was added into the mixture to prevent P1 *vir* reabsorption. Before plating on selection plates (LB agar plates supplemented with 5 mM Sodium citrate and 50 μg/mL kanamycin), 1 mL of LB was added into the transduction mixture and incubated at 37˚C for 1

hour to allow the expression of the newly transferred antibiotic resistance gene. Few transductants were picked and re-streak 2 times on LB plates containing kanamycin. Mutations were verified by PCR and agarose gel analysis. Correct transductants were kept in glycerol stock.

2.1.1.3 Removal of antibiotic resistance marker

Kanamycin resistance marker was excised from the mutant strains using pCP20 followed by loss of plasmid at the nonpermissive temperature. pCP20 is a temperature-sensitive plasmid which contains FLP recombinase gene, ampicillin resistance gene and chloramphenicol resistance gene. The Kan^R mutants were transformed with plasmid pCP20, and the chloramphenicol-resistant transformants were selected at 30˚C. Few colonies were re-streak on LB plates and incubated at 42˚C overnight to induce the expression of FLP recombinase and elimination of pCP20. Colonies losing all antibiotic resistances were selected and kept in glycerol stock.

2.1.2 Temperature-sensitive mutants

2.1.2.1 P1 donor lysate preparation

The procedure is the same as section 2.3.1.1 but with some modifications. The temperature used for cultivation is 30˚C for temperature sensitive strains. The mixture of bacteria and P1 *vir* was incubated at 30˚C for 30-40 min without shaking. After plating, the plates were incubated at 30˚C overnight.

2.1.2.2 P1 transduction

The details of P1 transduction is described in section 2.3.1.2. There are some modifications when constructing temperature-sensitive strains. The cultivation of recipient strain was carried out at 37˚C. The transduction was performed at 30˚C for 30-40 min without shaking. As temperature-sensitive donor strain carrying tetracycline resistance marker near to the point mutation, therefore, the transductants were selected from LB plates containing tetracycline at 30˚C. Few Tet^R transductants were re-streak on tetracycline plates and incubated at both permissive (30˚C) and nonpermissive temperature (42˚C) overnight. Tet^R colonies that show temperature-sensitive phenotype were selected, mutations were verified by PCR and sequencing. Correct mutants were kept in glycerol stock.

2.2 Plasmid construction and site-directed mutagenesis

The full-length *cydAB* gene together with its promoter region was amplified with

PrimeSTAR® Max using oligonucleotides cydABXE-EcoRI-F and cydABXE-BamHI-R. EcoRI-*cydABXE*-BamHI DNA fragment was ligated into the pBR322 vector, and resulting in pCYDAB (**Figure 2.1**). The correct DNA sequence of cloned *cydAB* in pCYDAB plasmid was confirmed by DNA sequencing. Amino acid substitutions were introduced by PrimeSTAR® Max with pCYDAB and synthetic oligonucleotides (Table 2.3) (**Figure 2.2**). Both Glu99 and Lys252 of CydA subunit were substituted with Ala (**Figure 2.3**), resulting in pCYDAB99 and pCYDAB252, respectively. Mutations were confirmed by DNA sequencing. The MK9313 strain was transformed with pCYDAB, pCYDAB99 or pCYDAB252 via electroporation for further experiments.

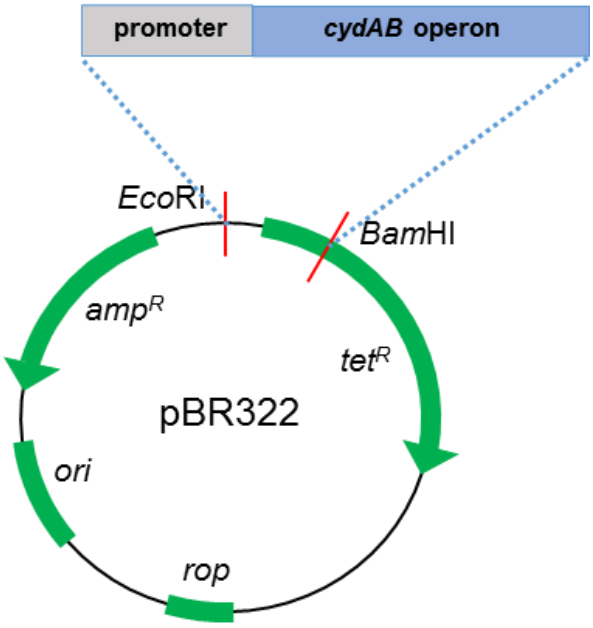

Figure 2.1 Plasmid structure of pCYDAB.

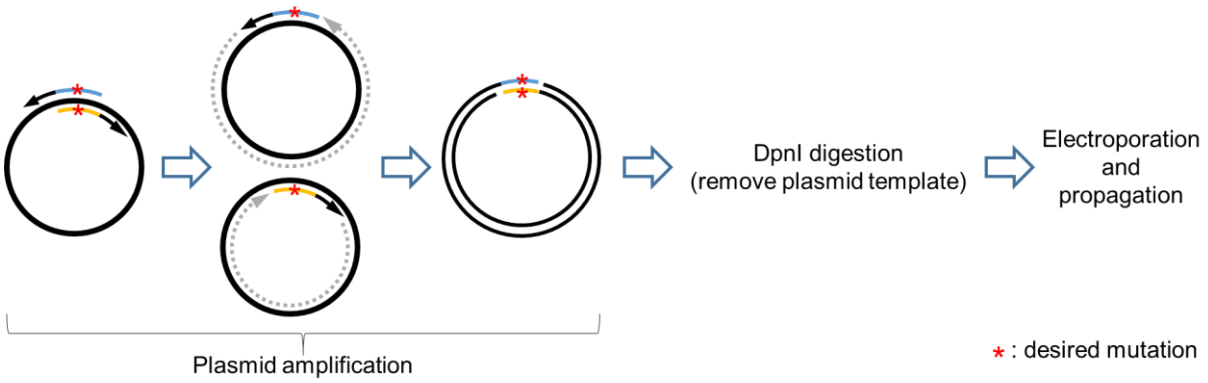

Figure 2.2 Construction of mutated plasmids (pCYDAB99 and pCYDAB252) by site-directed mutagenesis.

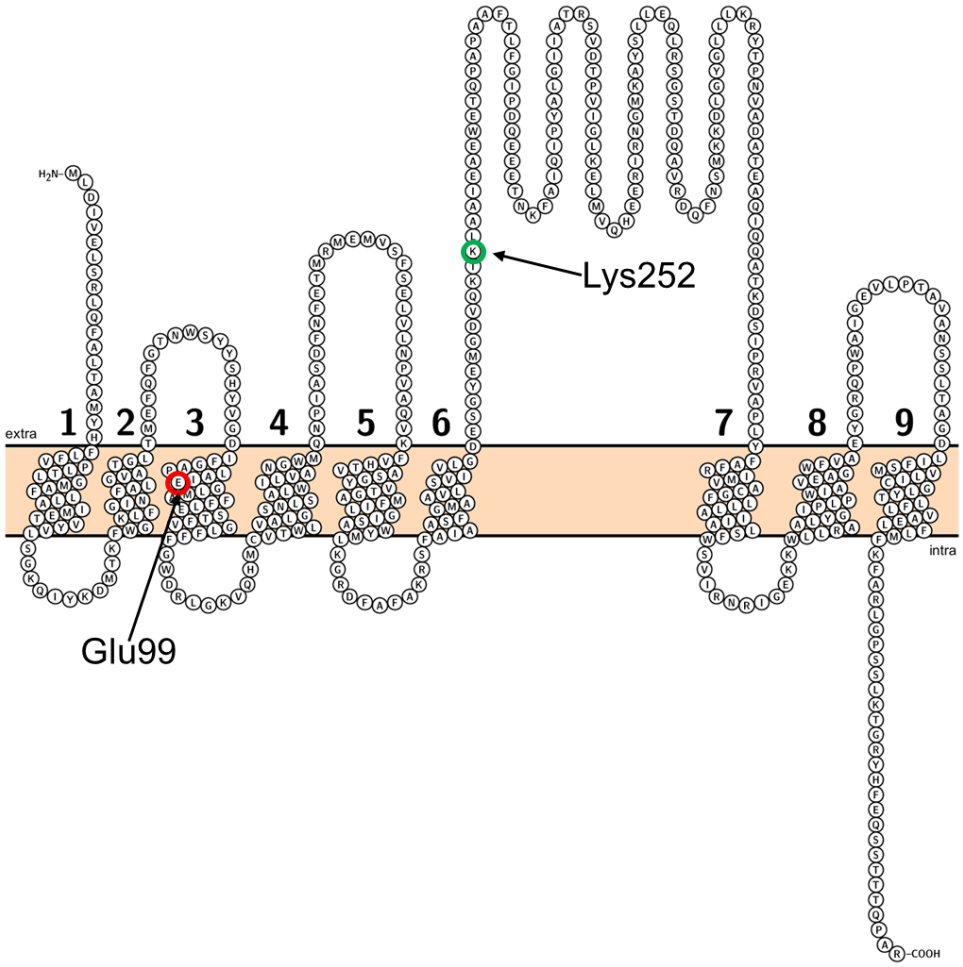

Figure 2.3 Topological model of CydA subunit. Glu99 (○) and Lys252 (○) were substituted with Ala, resulting in pCYDAB99 and pCYDAB252 respectively.

2.3 Generation of growth curve

Overnight culture was diluted with fresh medium at 1:100 and grown at 30˚C or 37˚C until OD_{600} reached 0.4. The exponentially growing culture was diluted to OD_{600} 0.01 prior to adding 100 mM hydroxyurea (HU) followed by incubation at 37˚C with 160 rpm shaking. For temperature-sensitive strains, OD_{600} 0.01 cultures were incubated at 30˚C or 42˚C with shaking. During the incubation, 200 µL of the culture was collected every 1 hour interval. OD_{600} values were measured at each time point. The collected samples were diluted, plated on LB agar and incubated at 30˚C or 37˚C for 18 hr or 14 hr, respectively. The total number of colonies were calculated and the mean value of at least three independent experiments was plotted.

2.4 Intracellular hydrogen peroxide and superoxide measurement

pTN247 and pTN249 plasmids were used to measure intracellular O_2^- level and H_2O_2 level, respectively. pTN247 plasmid contains *soxS*-GFP fusion gene whereas pTN249 contains *ahpC*-GFP fusion gene. The expression of *soxS*-GFP and *ahpC*-GFP fusion genes are regulated by intracellular O_2^- and H_2O_2 level, respectively.

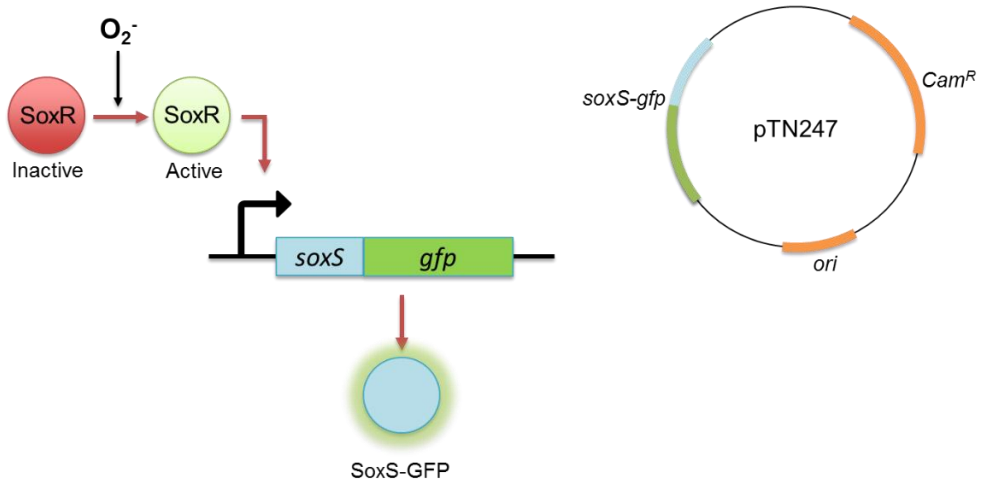

Figure 2.4 The GFP fluorescence intensity of cells harboring pTN247 reflects the intracellular superoxide level.

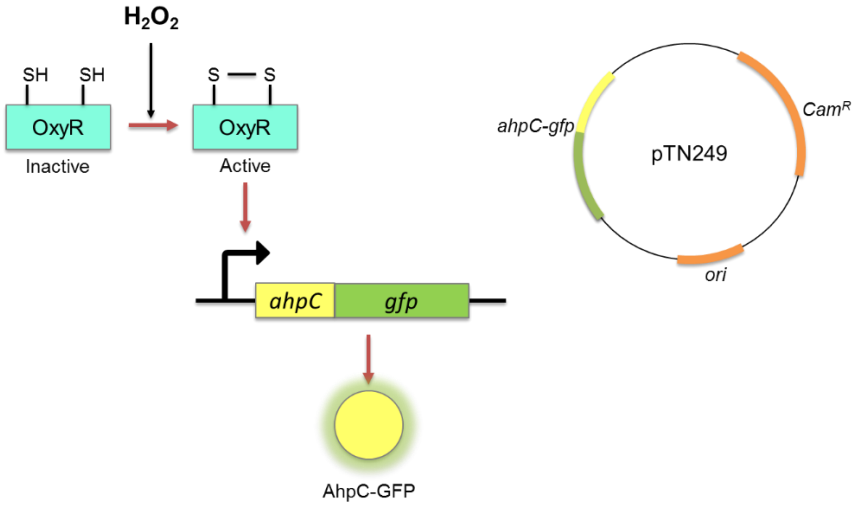

Figure 2.5 The GFP fluorescence intensity of cells harboring pTN249 reflects the intracellular hydrogen peroxide level.

Cells harboring GFP fusion plasmids were diluted in LB containing chloramphenicol and grown to exponential phase (OD_{600} 0.4) at 37˚C. The exponentially growing culture was further diluted to OD_{600} 0.01 in LB containing chloramphenicol with or without 100 mM HU.

A small amount of culture (200 µL) was collected at 0, 60 and 120 min. The collected samples were mixed with 2% sodium azide and then diluted with phosphate-buffered saline. The fluorescence signal must be detected within 20 min once the sodium azide was added. The fluorescence signal of the samples was collected using Accuri^{TM} C6 Flow Cytometer (BD) with a 488-nm argon laser and a 515- to 545-nm emission filter (FL1) at a low flow rate (Nakayashiki & Mori, 2013).

2.5 *rpoB* gene mutation assay

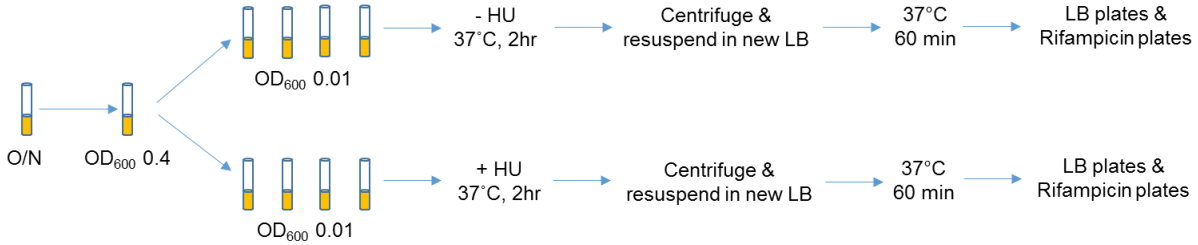

Figure 2.6 Mutation assay for HU-treated cells.

For HU treatment, the exponentially growing culture was diluted to OD_{600} 0.01 in 5 mL LB with or without 100mM HU. Cultures were grown at 37˚C with 160 rpm shaking speed for 2 hrs. Cultures were centrifuged and the pellets were resuspended with 5 mL LB. After growing the cells for another 1 hr at 37˚C, cells were collected by centrifuge at 5,000 rpm for 10 min. The cell pellets were resuspended with 500 µL LB. Diluted samples were plated on LB plates containing 100 µg/mL rifampicin at 37˚C to detect Rif^R colonies and on LB plates to determine viable cell titer. Colony counting was performed after 14 hrs for LB plates and 24 hrs for rifampicin plates.

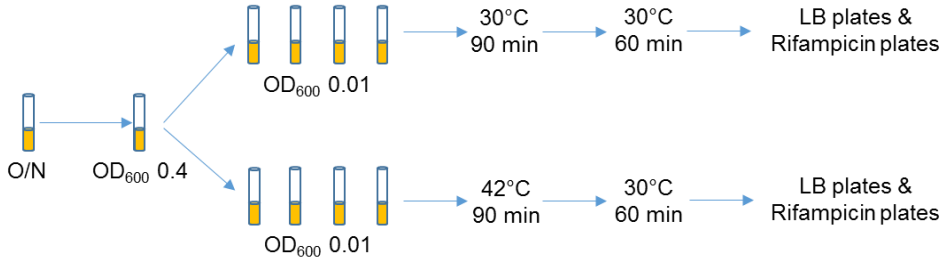

Figure 2.7 Mutation assay for temperature-sensitive *E. coli* strains.

For temperature-sensitive strain, cultures with OD_{600} 0.01 were grown at 30˚C and 42˚C for 90 min. After 90 min incubation, all cultures were grown at 30˚C for another 1 hr. Cells were collected by centrifugation and the pellets were resuspended with 500 µL LB. Diluted

samples were plated on LB plates with or without rifampicin and incubated at 30˚C. Colonies were scored after 18 hrs for LB plates and 28 hrs for rifampicin plates.

The Mutation frequency was determined by dividing the total number of Rif^R colonies to the total number of viable cells. Statistical evaluation (Paired T-test) was performed to evaluate differences between HU-treated and untreated cells or cells incubated at 30˚C and 42˚C.

2.6 Effect of iron chelator and hydroxyl radical scavenger on oxidative DNA damage

Sub-inhibitory concentrations of 2,2-bipyridine (250 μM; 50% MIC) and thiourea (100 mM; 50% MIC) were added to bacterial cultures 10 min prior to initiation of HU treatment. The cultures were then processed as for the *rpoB* gene mutation assays described above. For temperature-sensitive mutant, 250 μM of bipyridine and 60 mM of thiourea were added to the cultures 10 min prior to incubation at 42˚C.

Chapter 3 Results

Part 1. HU induces oxidative DNA damage in cells

1. HU induces hydroxyl radical-mediated oxidative DNA damage

Hydroxyl radical production has been shown to be a consequence of HU-induced DNA replication stress (Davies et al., 2009). Hydroxyl radical can lead to oxidative DNA damage in cells. However, there is no direct evidence to show that HU-induced hydroxyl radical formation can lead to oxidative DNA damage. To examine the correlation between HU treatment and oxidative DNA damage, I performed the *rpoB* gene mutation assay with HU-treated MK7180. All *E. coli* strains used in this study are strains carrying *mutM* and *mutY* double deletions. In *E. coli*, MutM and MutY are repair enzymes involved in protecting the cell from the mutagenic effects of 8-oxoG (Michaels et al., 1992; Tajiri et al., 1995). Thus, the mutation assay with strains carrying Δ*mutM* Δ*mutY* double deletions is a powerful tool to determine the oxidative DNA damage level in cells.

E. coli MK7180 (Δ*mutM* Δ*mutY*) strain was treated with 100 mM HU for 2 hours in liquid culture at OD_{600} 0.01. Since oxidative DNA damage leads to G:C to T:A mutations after two rounds of replication in Δ*mutM* Δ*mutY* strain, thus the cultures were incubated for another one-hour at 37°C after 2 hours of HU treatment (*Details of mutation assay on HU-treated cells are described in Chapter 2 section 2.5*). As shown in **Figure 3.1**, the average mutation frequency of HU-treated cells is ~4-fold higher compared to the untreated cells, indicating that HU-treated cells exhibit an increased level of oxidative DNA damages which probably due to the increased level of hydroxyl radical. In support of this conclusion, I observed that the addition of 100 mM thiourea completely reduced the oxidative DNA damages in HU-treated cells (**Figure 3.2**). Thiourea is a potent hydroxyl radical scavenger, which can react with hydroxyl radical and hence reduces the hydroxyl radicals that can damage the DNA. Since a high concentration of thiourea is toxic to the cells, the sub-lethal concentration of thiourea 100 mM was used in this study. Together, the results suggested that HU induces hydroxyl radical production and subsequently contributes to the production of oxidative DNA damages in cells.

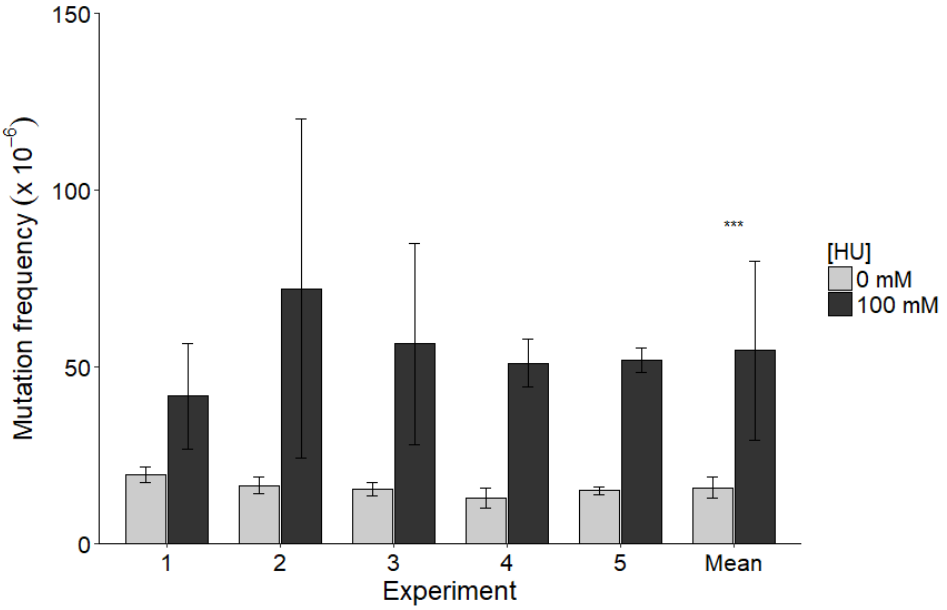

Figure 3.1 HU treatment increases oxidative DNA damage. Exponentially growing cultures were diluted to OD_{600} 0.01 and treated with 100 mM HU for 2 hours. Data points of each experiment represent the average of four replicas and the data point of mean represents the average of all five experiments. Error bars indicate standard deviation and (***) denotes p-value <0.001.

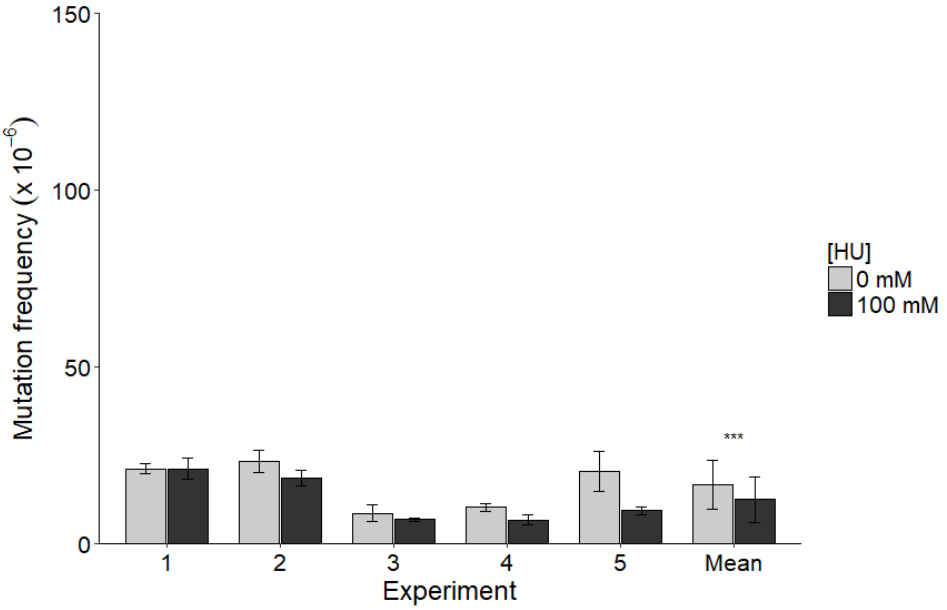

Figure 3.2 Thiourea suppresses the HU-induced oxidative DNA damage. Thiourea was added into MK7180 cultures 10 min prior to the HU treatment. Data points of each experiment represent the average of four replicas and the data point of mean represents the average of all five experiments. Error bars indicate standard deviation and the stars (***) indicate p-value <0.001.

2. HU induces cell death through the production of hydroxyl radicals

Previously, Collins and his colleagues reported that HU treatment induces hydroxyl radical-mediated cell killing in *E. coli* (Davies et al., 2009). In order to confirm their observation, I determined the growth curve of *E. coli* strain MK7180 treated with 100 mM HU in liquid culture (**Figure 3.3**). Cell growth was immediately ceased upon HU treatment and cells do not begin to die within the first hour. However, cell viability was declined dramatically after 2 hours of treatment and only ~ 0.2% of cells remained at 4-hours. Next, I examined the effect of hydroxyl radical scavenger thiourea to the growth of HU-treated culture. Addition of thiourea completely prevented the HU-induced cell death, whereas the HU-induced replication arrest is unaffected (**Figure 3.3**). These results supported the observation by the Collins group that HU treatment induces the formation of hydroxyl radicals, which can lead to cell death.

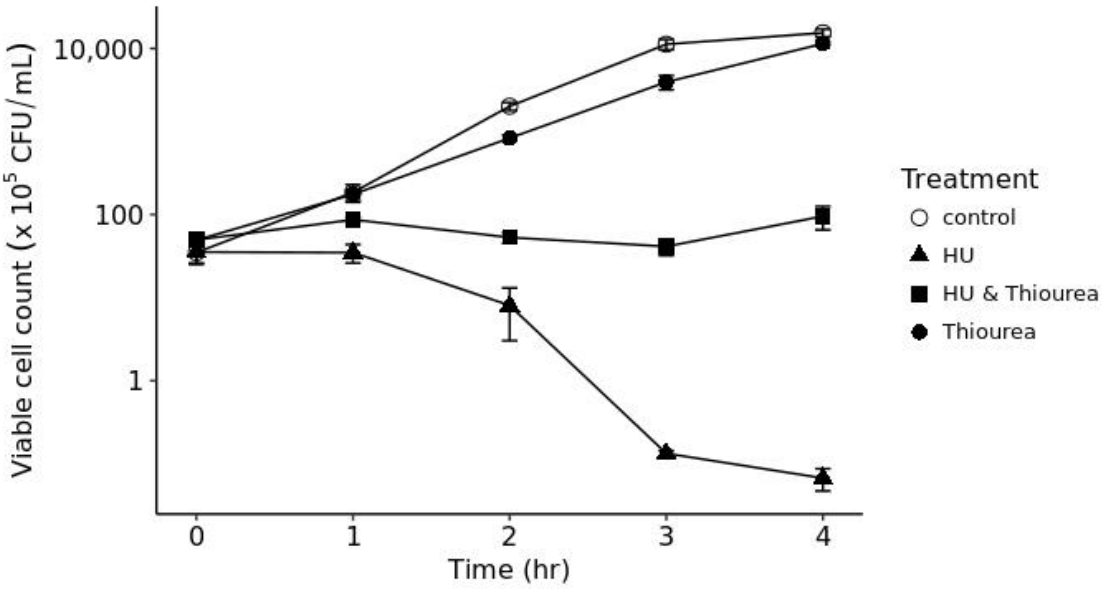

Figure 3.3 Growth curve of MK7180 treated with 100 mM HU in the presence (■) or absence (▲) of 100 mM thiourea. Exponentially growing cultures were diluted to OD_{600} 0.01 and treated with thiourea for 10 min prior HU treatment. Each data point represents the average of three independent experiments, and the error bars represent the standard deviation of the independent measurements.

Part 2. The molecular mechanism of HU-induced oxidative DNA damage

1. Toxin-antitoxin system and membrane stress response do not contribute to the cell death and oxidative DNA damage induction in HU-treated cells

Cell death in HU-treated cells has been reported as the downstream process that triggered by the toxin-antitoxin (TA) system and Cpx membrane stress-response two-component system (Davies et al., 2009; Godoy et al., 2006). In order to clarify whether the TA system and Cpx membrane stress system are involved in the HU-induced oxidative DNA damage, I examined the effects of TA system and Cpx membrane stress response system on the oxidative DNA damage in HU-treated cells.

TA systems are small genetic modules consisting of a stable toxin and its labile antitoxin. MazEF, a type II TA system in which the unstable MazE antitoxin binds and inhibits the MazF toxic activity. Without MazE antitoxin, MazF toxin blocks the protein synthesis by cleaving mRNAs specifically at ACA sites (Zhang et al., 2003). MazEF TA system has been shown to associate with programmed cell death in *E. coli* where *mazEF* deletion significantly increased the cell survival under ppGpp stress (Aizenman et al., 1996). **Figure 3.4** and **Figure 3.5** show the survival curve and mutation frequency of HU-treated MK7180Δ*mazF* strain, respectively. Contrary to the previously published result, deletion of *mazF* did not show any change in the cell viability upon HU treatment. On the other hand, *rpoB* gene mutation assay of MK7180Δ*mazF* strain revealed ~5-fold increase in mutation frequency upon 2 hours of HU treatment. Taken together, the results demonstrated that neither HU-induced cell death nor HU-induced oxidative DNA damages requires the MazEF TA system.

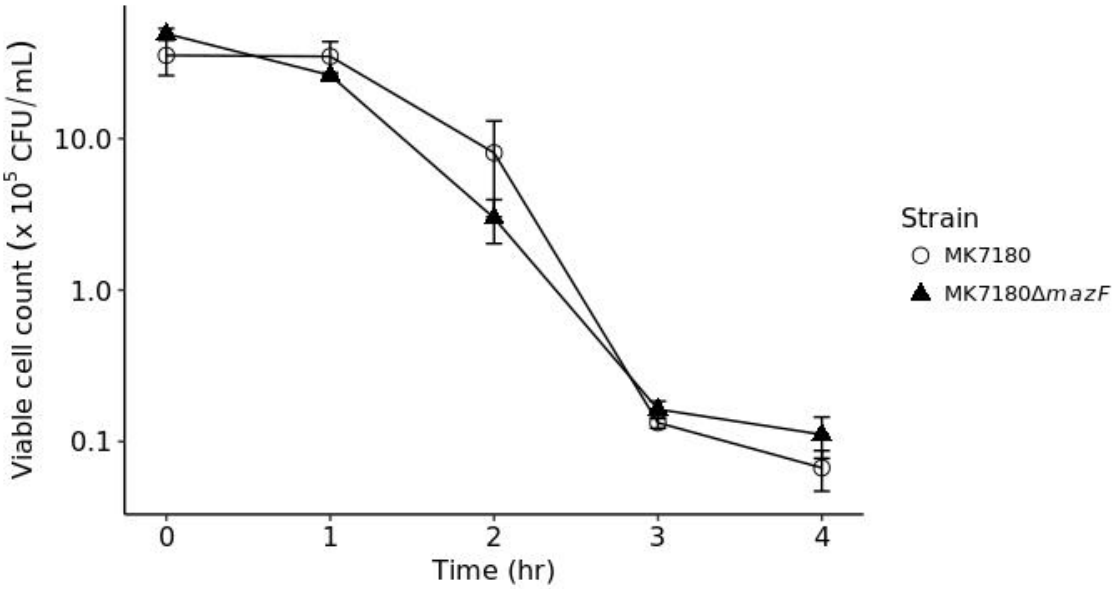

Figure 3.4 Deletion of *mazF* does not affect the cell survival rate in HU-treated cells. MK7180 (○) and MK7180Δ*mazF* (▲) were treated with 100 mM HU. Each data point represents the average of three independent experiments, and the error bars represent the standard deviation of the independent measurements.

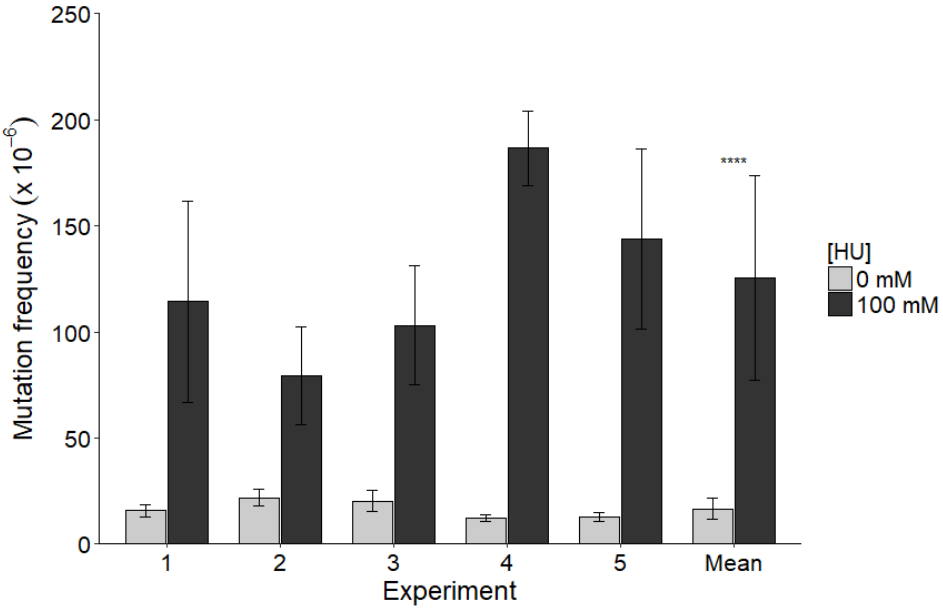

Figure 3.5 HU-induced oxidative DNA damage occurs in the absence of MazF toxin. This experiment was performed by using MK7180Δ*mazF*. Data points of each experiment represent the average of four replicas and the data point of mean represents the average of all five experiments. Error bars indicate standard deviation and the stars (****) indicate p-value <0.0001.

Besides the TA system, Cpx membrane stress response system has been suggested to play a role in bactericidal antibiotic-mediated cell death as well as HU-induced cell death (Davies et al., 2009; Kohanski et al., 2008). In *E.coli*, the Cpx two-component system comprises the membrane-associated CpxA sensor kinase/phosphatase and the CpxR response regulator (Raivio & Silhavy, 1997). CpxA responses to the environmental stresses, especially protein misfolding near the membrane and periplasm, via autophosphorylation and subsequently phosphotransfer to the CpxR. Activated CpxR functions as a transcriptional activator of genes which encode proteins involved in protein folding and degradation (Pogliano et al., 1997). In this study, I observed no significant difference in the cell viability of HU-treated MK7180Δ*cpxA* strain compared to HU-treated MK7180 (**Figure 3.6**). Deletion of *cpxA* did not prevent the HU-induced cell death. Mutation frequency of MK7180Δ*cpxA* also did not show significant change as compared to the wild-type MK7180 strain (**Figure 3.7**). In summary, these results indicated that the Cpx membrane stress response system is not involved in HU-induced cell death and HU-induced oxidative DNA damage.

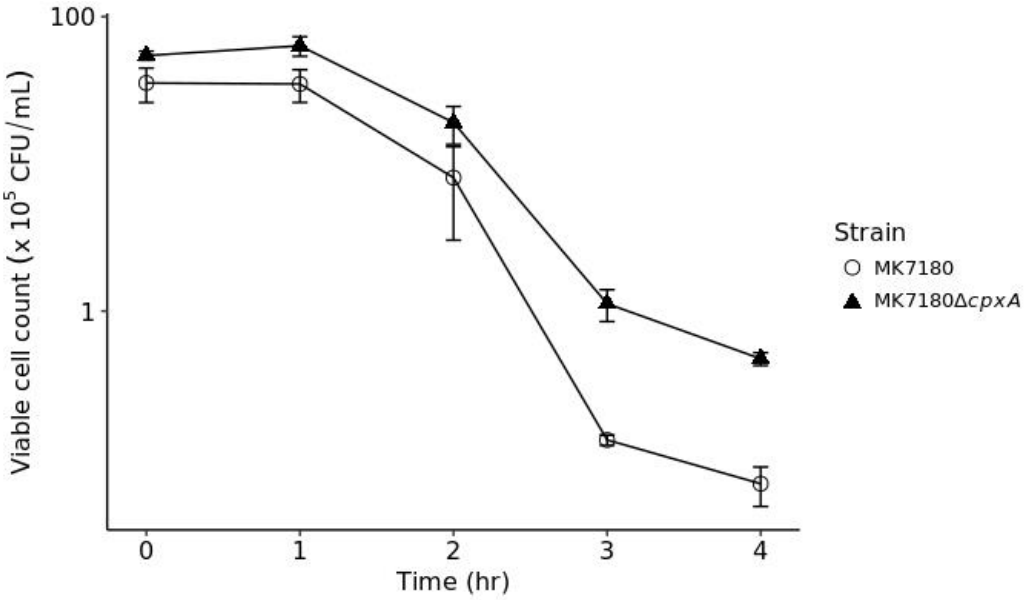

Figure 3.6 Deletion of *cpxA* does not prevent HU-induced cell death. MK7180 (○) and MK7180Δ*cpxA* (▲) treated with 100 mM HU. Each data point represents the average of three independent experiments, and the error bars represent the standard deviation of the independent measurements.

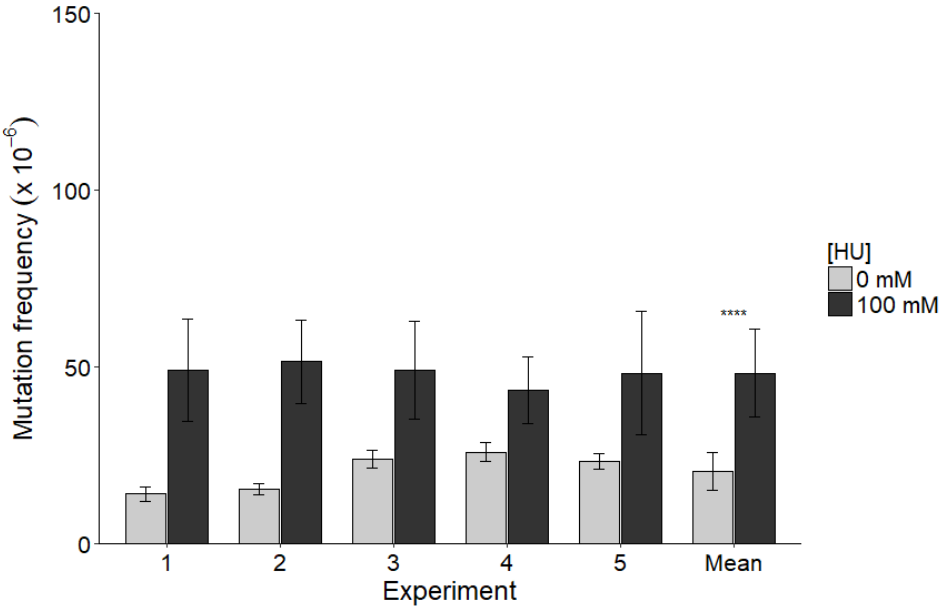

Figure 3.7 Disruption of Cpx membrane stress response system has no effects on HU-induced oxidative DNA damages. MK7180Δ*cpxA* strain was used in this experiment. Data points of each experiment represent the average of four replicas and the data point of mean represents the average of all five experiments. Error bars indicate standard deviation and the stars (****) indicate p-value <0.0001.

2. Disruption of cytochrome oxidase *bd*-I suppresses HU-induced cell death and oxidative DNA damage

Based on the previous studies, the lethality of temperature-sensitive polymerase III mutant and HU-treated cells can be prevented by disrupting the cytochrome oxidase *bd*-I (Davies et al., 2009; Strauss et al., 2004). By treated the cultures with 100 mM HU, I observed that deletion of *cydAB* genes, which encode cytochrome oxidase *bd*-I complex, completely suppressed both HU-induced cell death and HU-induced oxidative DNA damage (**Figure 3.8 & 3.9**). The viable cell count of MK7180Δ*cydAB* did not show a significant change even though treated with HU for 4 hours (**Figure 3.8**). Furthermore, the mutation frequency of HU-treated MK7180Δ*cydAB* was similar to those in untreated cells (**Figure 3.9**), suggesting that the addition of HU did not cause further production of oxidative DNA damages in cells.

Besides the cytochrome oxidase *bd*-I, *E. coli* contains another two major terminal oxidases in the aerobic respiration chain: cytochrome oxidase *bo* (*cyoABCD*) and *bd*-II (*cbdAB*). Similarly to wild-type MK7180, the mutation frequency of HU-treated MK7180Δ*cyoABCD* and MK7180Δ*cbdAB* were approximately 4-fold higher compared to untreated cells (**Figure 3.10 & 3.11**).

The results demonstrated that only cytochrome oxidase *bd*-I is responsible for the oxidative DNA damages and cell death in HU-treated cells.

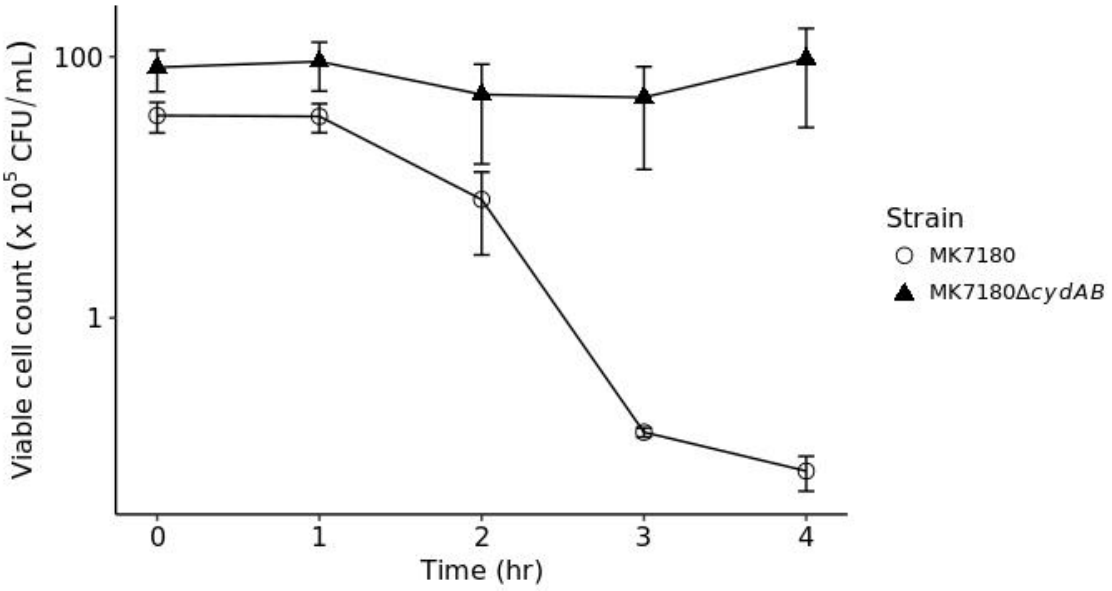

Figure 3.8 Deletion of *cydAB* completely suppresses the cell killing effect of HU. MK7180 (○) and MK7180Δ*cydAB* (▲) were treated with 100 mM HU. Each data point represents the average of three independent experiments, and the error bars represent the standard deviation of the independent measurements.

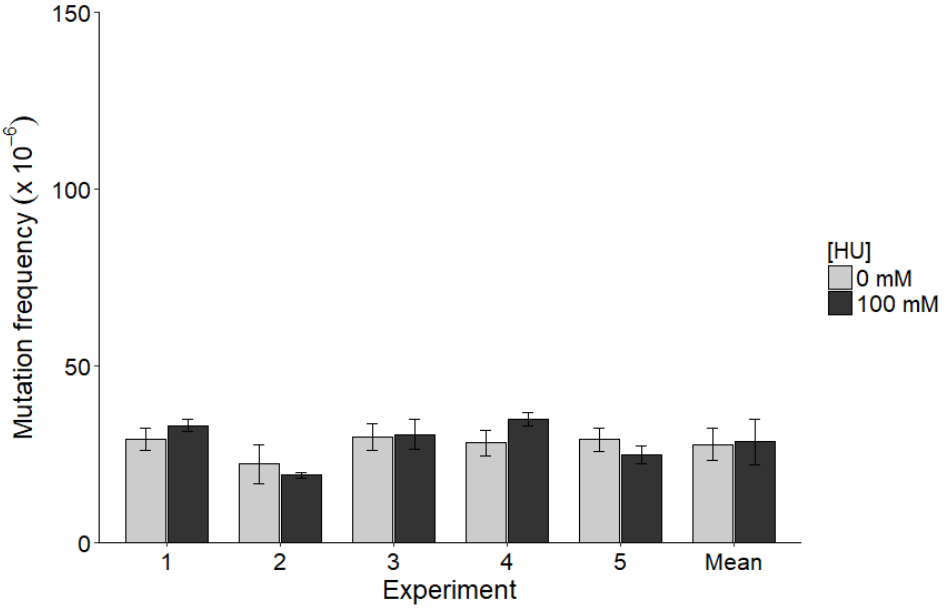

Figure 3.9 Absence of cytochrome oxidase *bd*-I completely suppresses HU-induced oxidative DNA damages. MK7180Δ*cydAB* was used in this experiment. Data points of each experiment represent the average of four replicas and the data point of mean represents the average of all five experiments. Error bars indicate standard deviation.

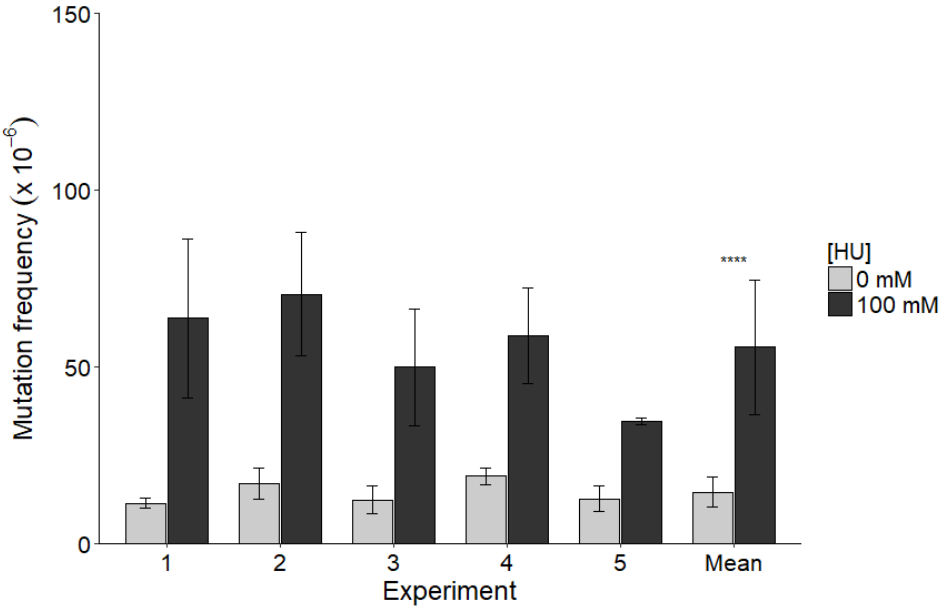

Figure 3.10 Cytochrome oxidase *bo* is not involved in HU-induced oxidative DNA damages. MK7180Δ*cyoABCD* was used in this experiment. Data points of each experiment represent the average of four replicas and the data point of mean represents the average of all five experiments. Error bars indicate standard deviation and the stars (****) indicate p-value <0.0001.

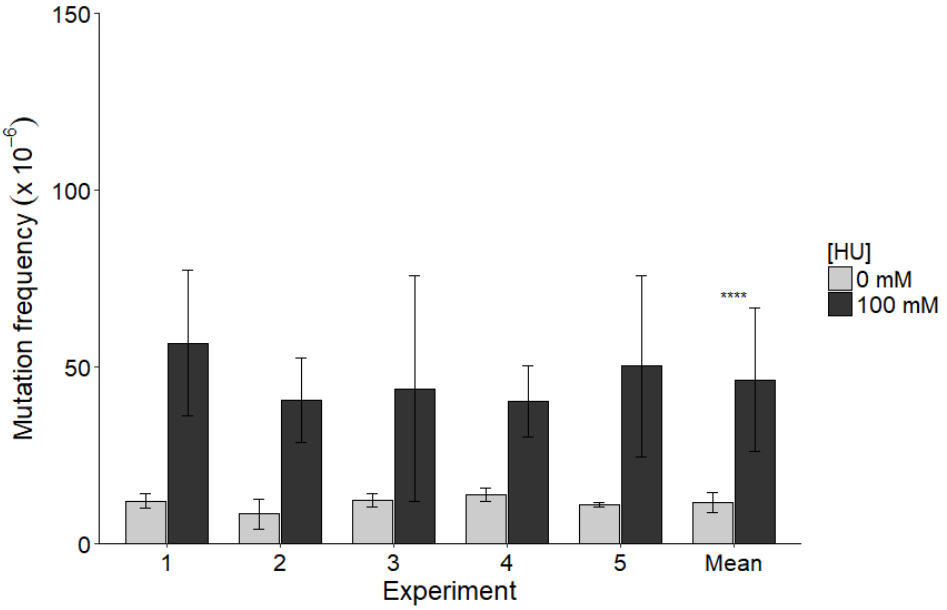

Figure 3.11 Disruption of cytochrome oxidase *bd*-II does not reduce the oxidative DNA damage in HU-treated cells. This experiment was done by using MK7180Δ*cbdAB* strain. Data points of each experiment represent the average of four replicas and the data point of mean represents the average of all five experiments. Error bars indicate standard deviation and the stars (****) indicate p-value <0.0001.

3. HU treatment affects the intracellular ferrous ion level

The main source of intracellular ROS is the respiratory chain. Inappropriate reduction of oxygen molecules can result in superoxide production (Imlay & Fridovich, 1991). Superoxide will subsequently change to H_2O_2 and finally to hydroxyl radicals when H_2O_2 react with free ferrous ion (Fe^{2+}). HU treatment has been proposed to trigger a series of downstream process that disrupts the action of cytochrome oxidase *bd*-I in the electron transport chain and causes inappropriate releasing of superoxide (Davies et al., 2009).

In order to monitor the superoxide production in HU-treated cells, I used pTN247 plasmid which contains *soxS* native promoter and the N-terminal region of *soxS* gene that fused with GFP (Nakayashiki & Mori, 2013). The expression of GFP is fully dependent on the transcription of *soxS* gene and correlates with the level of intracellular superoxide. The expression of *soxS-gfp* fusion gene was detected and quantified by flow cytometry. The result showed that GFP intensity was increased upon HU treatment with the higher value of 4,700, corresponding to 2-fold value of untreated cells at 2-hour time point (**Figure 3.12**). Next, I examined the H_2O_2 formation in HU-treated cells by using the pTN249 plasmid, which contains the *ahpC-gfp* fusion gene (Nakayashiki & Mori, 2013). The GFP intensity also increased upon HU treatment (**Figure 3.13)**. These results suggested that HU treatment does slightly increase the intracellular superoxide and H_2O_2 levels.

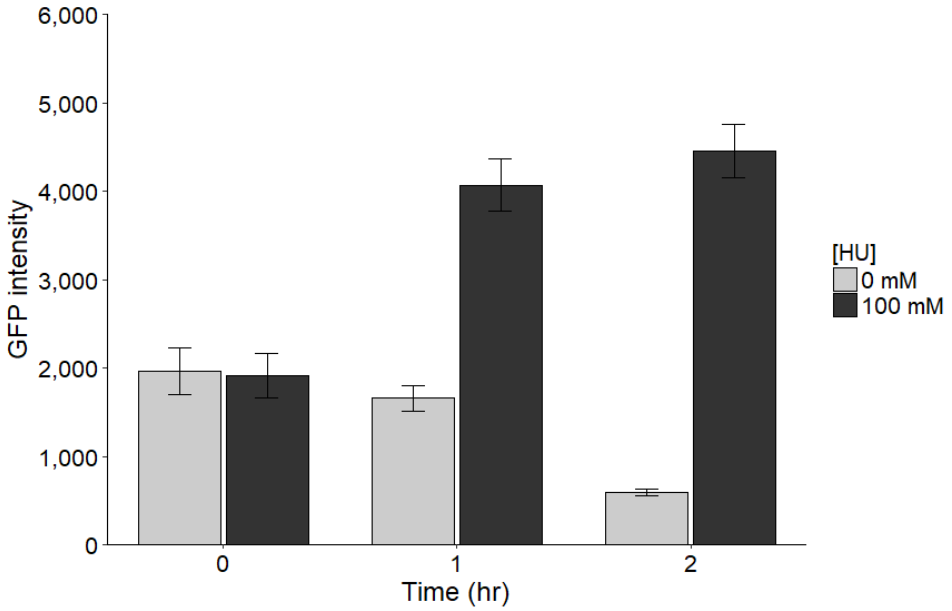

Figure 3.12 Intracellular superoxide level in HU-treated MK7180. The data were obtained from six independent experiments. Error bars indicate the standard deviation of the independent measurements.

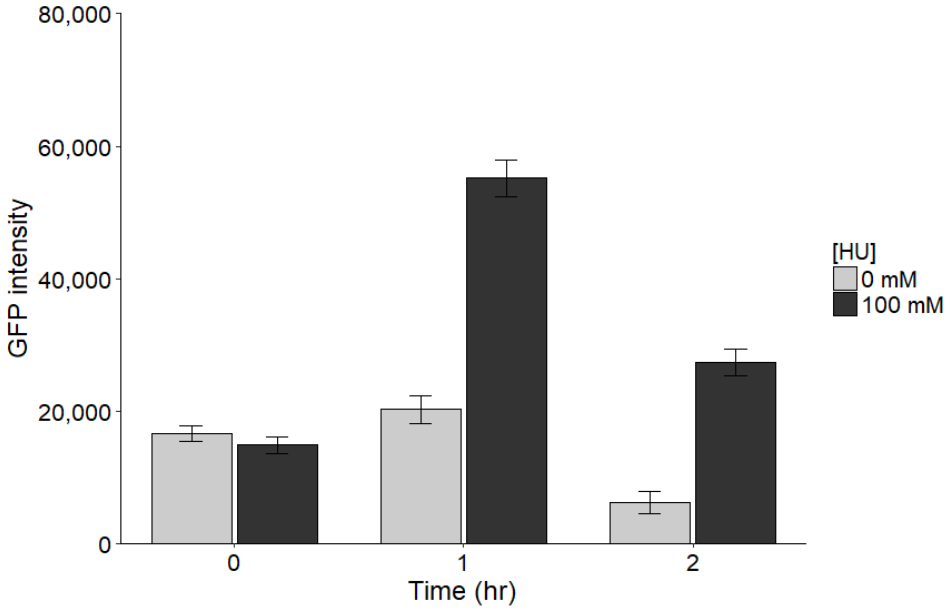

Figure 3.13 Intracellular H_2O_2 level in HU-treated MK7180. The data were obtained from five independent experiments. Error bars indicate the standard deviation of the independent measurements.

A speculation that cytochrome oxidase *bd*-I is responsible for the superoxide production in HU-treated cells was previously proposed (Davies et al., 2009). However, I found that deletion of *cydAB* genes, which encode cytochrome oxidase *bd*-I complex, did not suppress the superoxide or H_2O_2 production (**Figure 3.14 & 3.15**). Formation of hydroxyl radical depends on the cellular H_2O_2 and Fe^{2+} ion (**Figure 1.1**). Therefore, I hypothesized that intracellular Fe^{2+} level might be affected by HU. To check the involvement of Fe^{2+} in HU-induced cell death and oxidative DNA damages, I treated the MK7180 cells with sub-lethal concentration of iron chelator 2,2'-bipyridine. Bipyridine reacts with free Fe^{2+} to form complexes and hence reduces the free Fe^{2+} molecules that are available for hydroxyl radical formation. The sub-lethal concentration of bipyridine led to a complete suppression of HU-induced oxidative DNA damage (**Figure 3.16**), suggesting that Fe^{2+} is involved in the HU-induced oxidative DNA damage. The addition of iron chelator also partially prevent HU-induced cell death (**Figure 3.17**). These results suggested that Fe^{2+} plays a role in HU-induced oxidative DNA damage and HU-induced cell death.

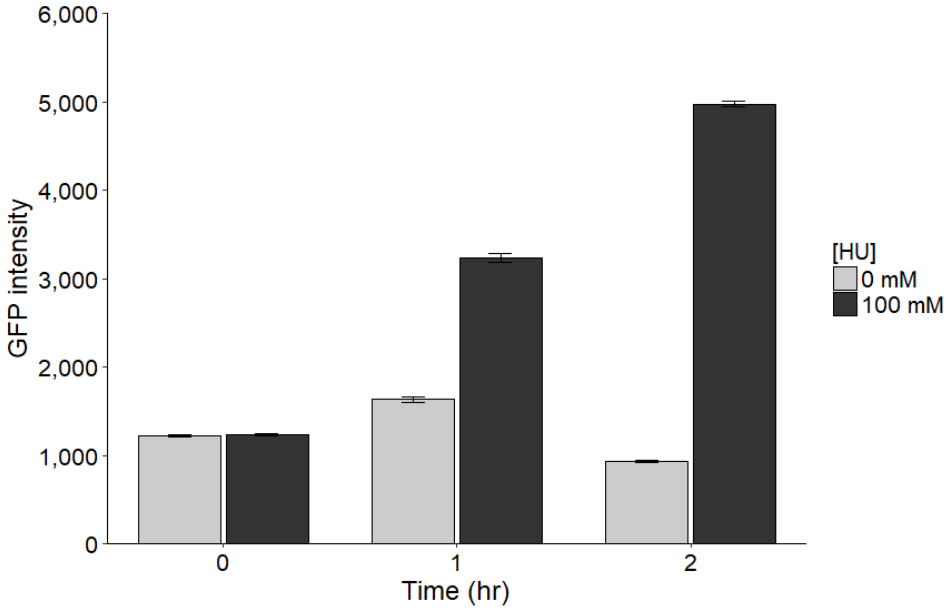

Figure 3.14 Intracellular superoxide level in HU-treated MK7180Δ*cydAB*. The data were obtained from three independent experiments. Error bars indicate the standard deviation of the independent measurements.

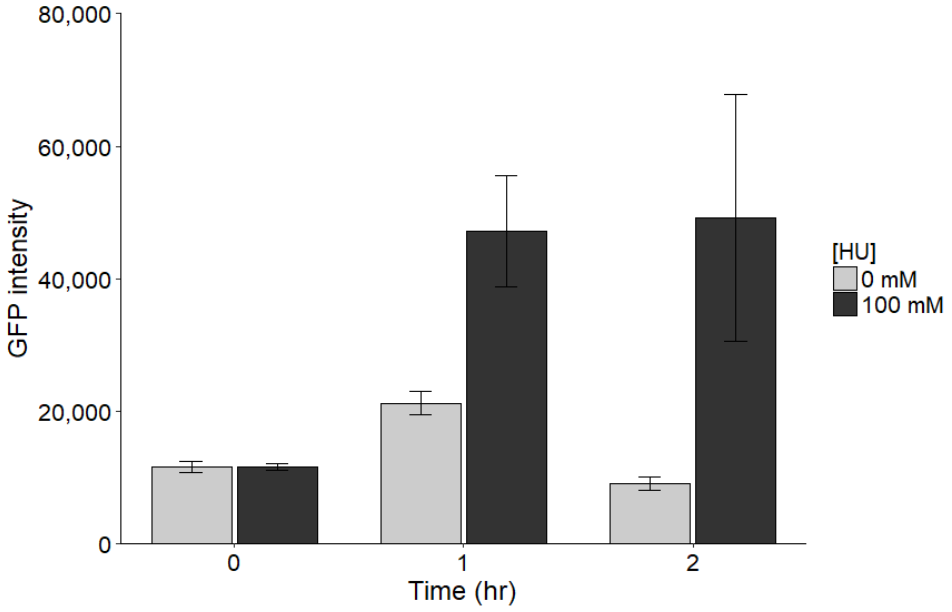

Figure 3.15 Intracellular H_2O_2 level in HU-treated MK7180Δ*cydAB*. The data were obtained from six independent experiments. Error bars indicate the standard deviation of the independent measurements.

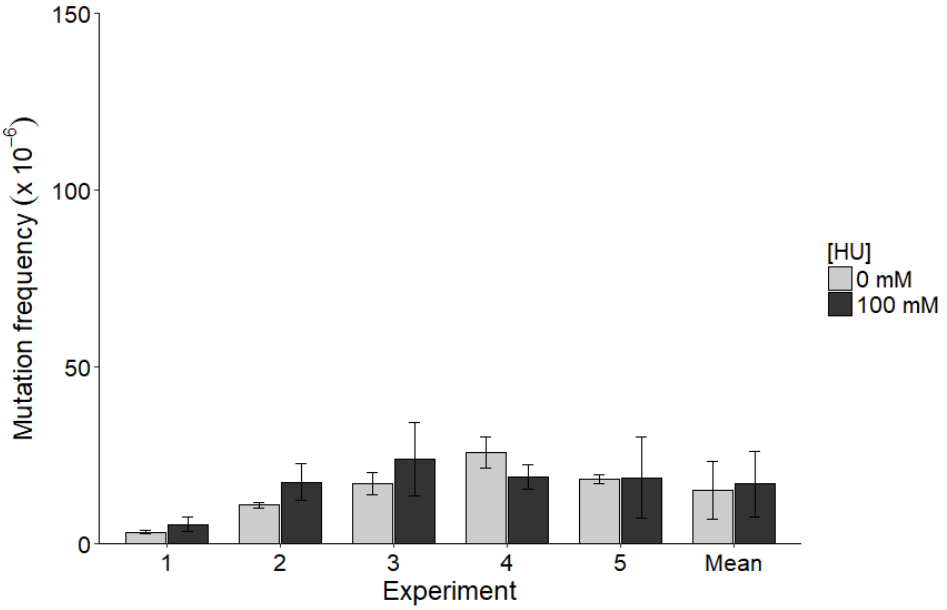

Figure 3.16 Bipyridine suppresses the HU-induced oxidative DNA damages. Bipyridine was added into MK7180 cultures 10 min before HU treatment. Data points of each experiment represent the average of four replicas and the data point of mean represents the average of all five experiments. Error bars indicate standard deviation.

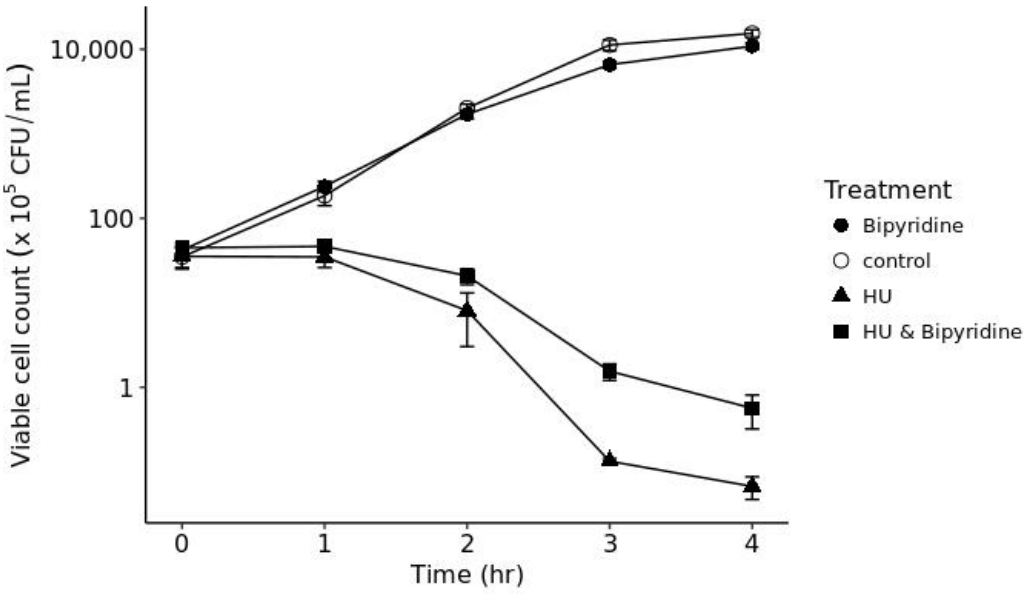

Figure 3.17 Survival curve of MK7180 treated with 100 mM HU in the presence (■) or absence (▲) of 0.2 mM bipyridine. Exponentially growing cultures were diluted to OD600 0.01 and treated with bipyridine for 10 min before HU was added. Each data point represents the average of three independent experiments, and the error bars represent the standard deviation of the independent measurements.

4. Oxidase activity of cytochrome oxidase *bd*-I is not required for HU-induced cell death and oxidative DNA damage

I have proved that the disruption of cytochrome oxidase *bd*-I completely suppressed HU-induced cell death and oxidative DNA damages. Since cytochrome oxidase *bd*-I is a heme-containing enzyme, it is possible that heme from the cytochrome oxidase *bd*-I becomes the source of Fe^{2+} that causes oxidative DNA damage and cell death upon HU treatment. To test this hypothesis, first I constructed three different plasmids: plasmid carrying the wild-type *cydAB* (pCYDAB), plasmid carrying *cydAB* with E99A substitution (pCYDAB99) and plasmid carrying *cydAB* with K252A substitution (pCYDAB252) (*Details of plasmid constructions and site-directed mutagenesis are described in Chapter 2 section 2.2)*. Glutamate at position 99 (Glu99) in CydA subunit is essential for the binding of heme and enzymatic activity (Mogi, Endou, et al., 2006). Whereas Lysine at position 252 (Lys252), located in the Q-loop, involved in the quinol oxidation by cytochrome oxidase *bd* (Mogi, Mizuochi-Asai, et al., 2006). Replacement of Glu99 with Ala (E99A) reduced the heme content and the oxidase activity remains approximately 13%. Recently, there is another publication reporting that E99A substitution reduced 50% of heme d and 72% of the enzymatic activity is remained (Murali & Gennis, 2018). On the other hand, substitution of Lys252 with Ala (K252A) reduced the oxidase activity to 3.5% but the heme content remains unchanged (Mogi, Endou, et al., 2006). Upon HU treatment, MK9313 (MK7180Δ*cydAB*) carrying pCYDAB99 did show a significant suppression of HU-mediated cell killing when compared to MK9313 carrying pCYDAB (**Figure 3.18**). In contrast, the presence of pCYDAB252 did not prevent HU-induced cell death (**Figure 3.18**). Moreover, pCYDAB99 rather than pCYDAB252 suppressed the HU-induced oxidative DNA damages (**Figure 3.19, 20 & 3.21**). Altogether, these results clearly suggested that HU-induced cell death and oxidative DNA damage did not require the oxidase activity of cytochrome oxidase *bd*-I.

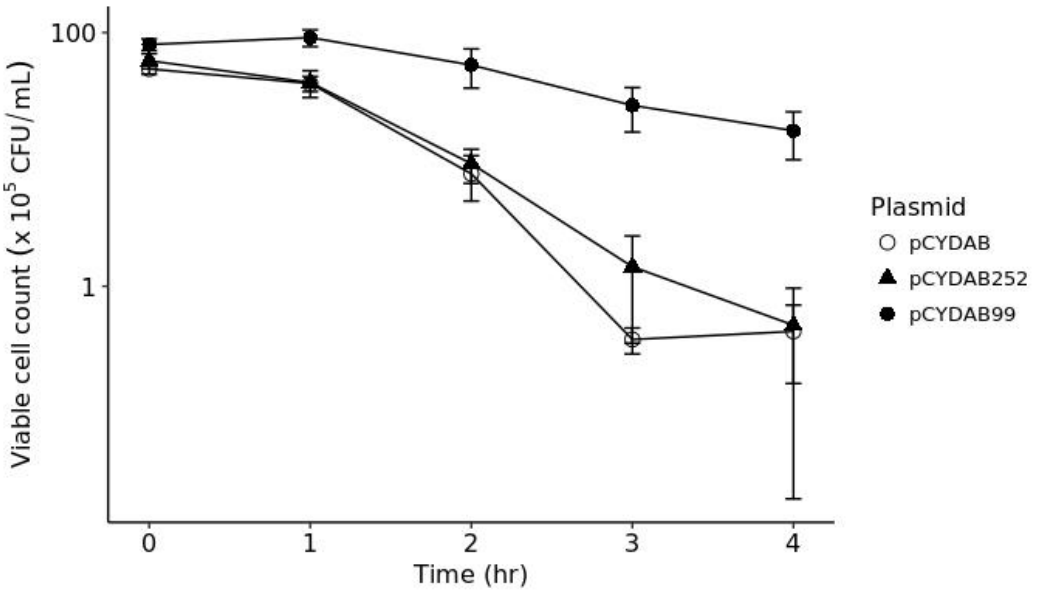

Figure 3.18 Survival curve of HU-treated MK9313 harboring either wild-type or mutated *cydAB* plasmids. MK9313 harboring either pCYDAB (○), pCYDAB99 (●) or pCYDAB252(▲) were treated with 100 mM HU. Each data point represents the average of three independent experiments, and the error bars represent the standard deviation of the independent measurements.

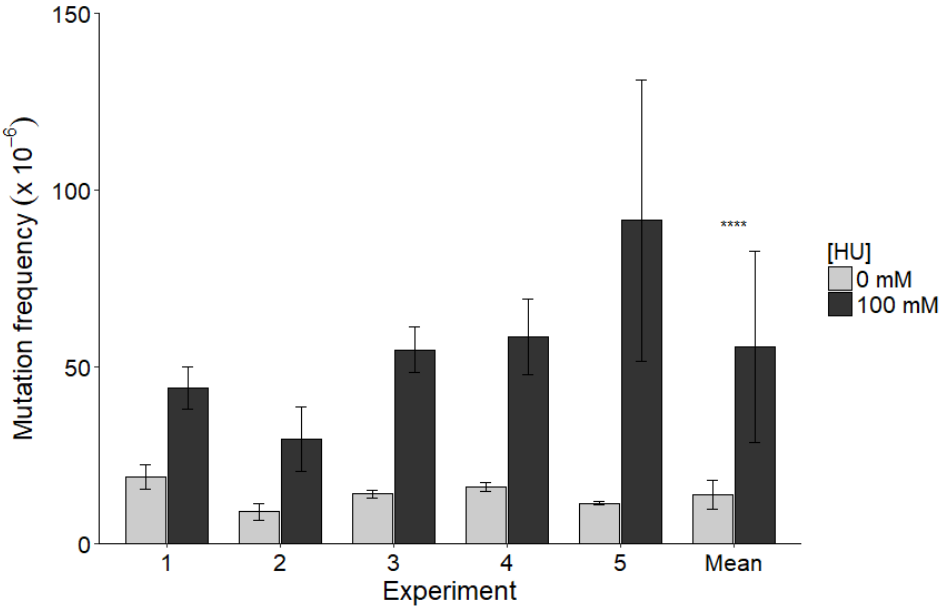

Figure 3.19 Mutation frequency of MK9313 carrying pCYDAB. pCYDAB carrying wild-type *cydAB* operon. Data points of each experiment represent the average of four replicas and the data point of mean represents the average of all five experiments. Error bars indicate standard deviation and the stars (****) indicate p-value <0.0001.

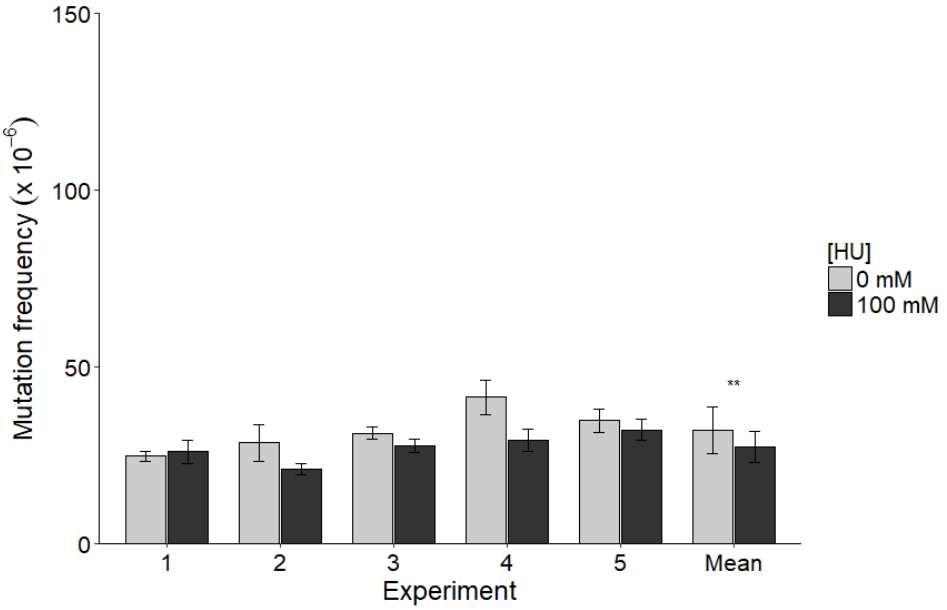

Figure 3.20 The presence of pCYDAB99 in MK9313 suppresses HU-induced oxidative DNA damages. pCYDAB99 carrying *cydAB* operon with an amino acid substitution at position 99 in CydA subunit. Data points of each experiment represent the average of four replicas and the data point of mean represents the average of all five experiments. Error bars indicate standard deviation and the stars (**) indicate p-value <0.01.

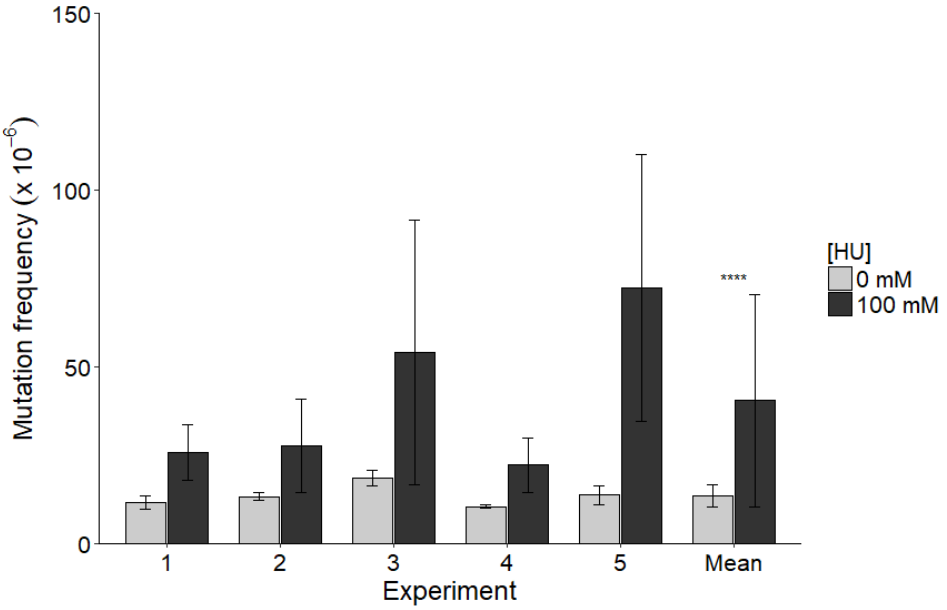

Figure 3.21 The presence of pCYDAB252 in MK9313 does not suppress HU-induced oxidative DNA damages. pCYDAB252 carrying a *cydAB* gene with an amino acid substitution at position 252 in CydA subunit. Data points of each experiment represent the average of four replicas and the data point of mean represents the average of all five experiments. Error bars indicate standard deviation and the stars (****) indicate p-value <0.0001.

Part 3. Induction of oxidative DNA damage in strains defective in DNA replication machinery

1. Oxidative DNA damage in temperature-sensitive Pol III mutant increases at non-permissive temperature

To clarify whether the mechanism of HU-induced oxidative DNA damage can be generalized to other DNA replication stress condition, I determined the growth curve and mutation frequency of temperature-sensitive *dnaE* mutants, *dnaE486*, at permissive and non-permissive temperatures. The *dnaE* gene encodes the alpha-catalytic subunit of DNA polymerase III (Pol III) which is essential for DNA synthesis in *E. coli. dnaE486*(ts) mutant contains a single base-pair missense mutation at 2653nt (T to C) which results in S885P substitution. Incubation at non-permissive temperature can lead to DNA replication arrest in *dnaE486*(ts) mutant (Vandewiele et al., 2002).

In order to examine the effects of DNA replication arrest in *dnaE486*(ts) mutant, the cells were incubated either at 30°C or 42°C for 1.5 hrs (*Details of growth curve generation and mutation assay on dnaE486 mutant are described in Chapter 2 section 2.3 and 2.5*). At the permissive temperature of 30°C, the viable cell number of *dnaE486*(ts) mutant was logarithmically increasing. *dnaE486*(ts) mutant quickly stopped the cell division but not exhibited a significant change in the cell viability within the first hour of incubation at 42°C. However, it did show a dramatic decrease in viable cell count after 1 hour of incubation (**Figure 3.22**). Cell viability of *dnaE486*(ts) mutant declined to ~1% by 2 hours incubation at 42°C. In contrast to the HU-induced cell killing, as shown in **Figure 3.22**, no difference was observed in the cell viability at 42°C when 60 mM thiourea-treated and untreated cells were compared.

Similarly to the HU-treated cells, Δ*mutM* Δ*mutY dnaE486*(ts) mutant resulted in higher mutation frequency at 42°C (**Figure 3.23**). I also found that the mutation frequency of temperature-sensitive strain defective in helicase B (*dnaB42*) with Δ*mutM* Δ*mutY* was increased when cells were incubated at 42°C (**Figure 3.25**). These observations indicated that cells under DNA replication stress exhibit increased level of oxidative DNA damage which probably due to the increased level of hydroxyl radical. In support of this conclusion, I observed that the addition of thiourea completely reduced the mutation frequency of *dnaE486*(ts) mutant at 42°C (**Figure 3.24**). Together, these results clearly indicated that inactivation of Pol III induces hydroxyl radical production and subsequently lead to oxidative DNA damages. However, hydroxyl radical production is not the cause of cell death in *dnaE486*(ts) mutant.

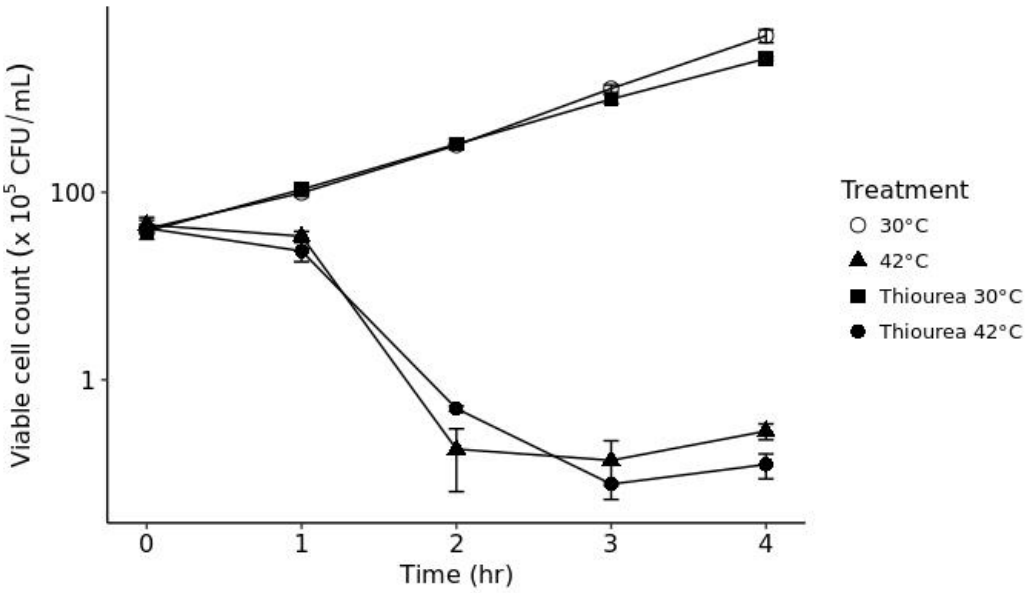

Figure 3.22 Survival curve of MK7180*dnaE486*(ts) grown at non-permissive temperature (42°C) in the presence (●) or absence (▲) of 60 mM thiourea. Exponentially growing cultures were diluted to OD_{600} 0.01 and treated with thiourea for 10 min prior to transfer to 42°C. Each data point represents the average of three independent experiments, and the error bars represent the standard deviation of the independent measurements.

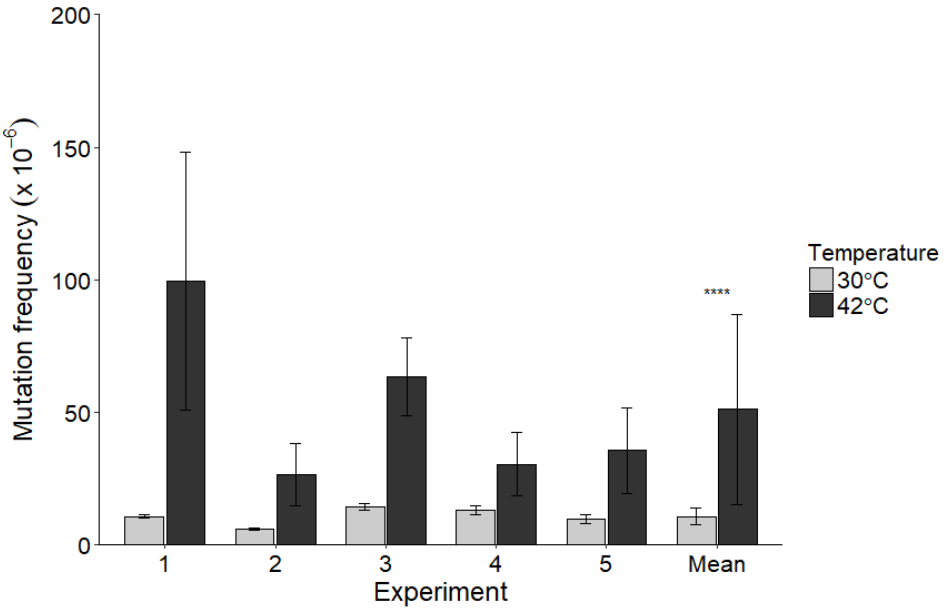

Figure 3.23 Malfunction of polymerase III increases oxidative DNA damages. Mutation frequencies were determined after 1.5 hours incubation at 30°C or 42°C. This experiment was performed by using MK7180*dnaE486*(ts) strain. Data points of each experiment represent the average of four replicas and the data point of mean represents the average of all five experiments. Error bars indicate standard deviation and the stars (****) indicate p-value <0.0001.

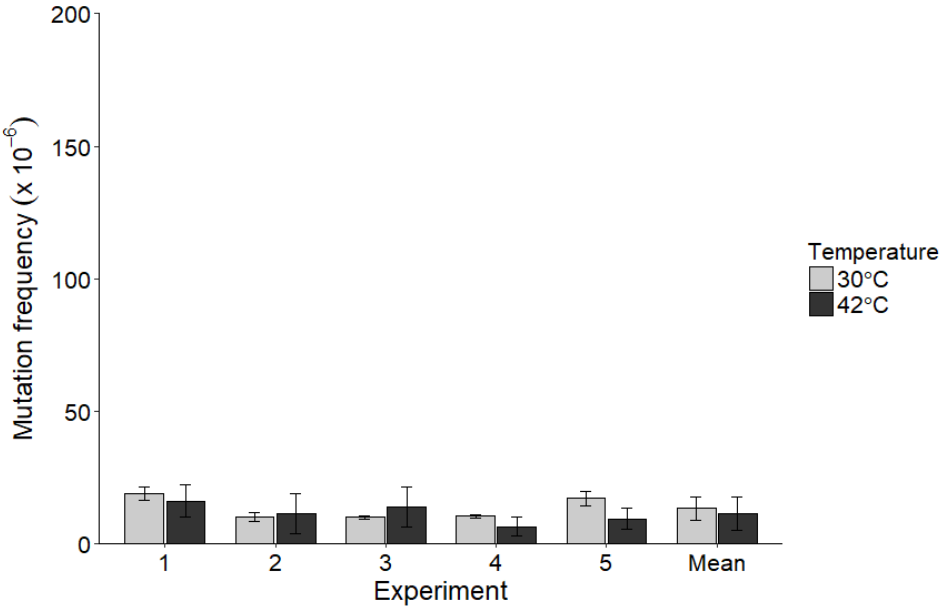

Figure 3.24 Thiourea suppresses oxidative DNA damages in MK7180*dnaE486*(ts) at non-permissive temperature. Data points of each experiment represent the average of four replicas and the data point of mean represents the average of all five experiments. Error bars indicate standard deviation.

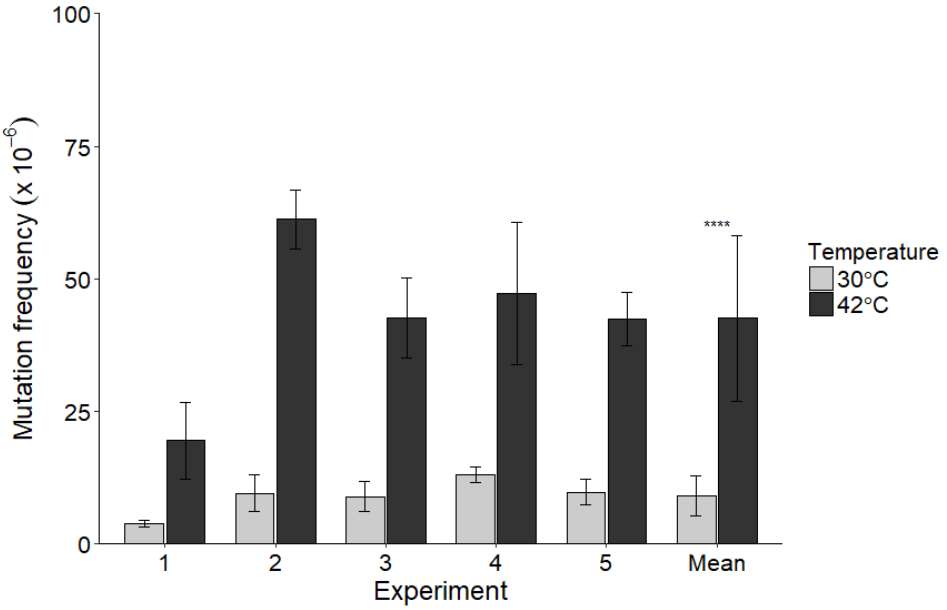

Figure 3.25 Malfunction of DnaB helicase increases oxidative DNA damages. Mutation frequencies were determined after 1.5 hours of incubation at non-permissive temperature. This experiment was performed by using MK7180*dnaB42*(ts) strain. Data points of each experiment represent the average of four replicas and the data point of mean represents the average of all five experiments. Error bars indicate standard deviation and the stars (****) indicate p-value <0.0001.

2. Induction of oxidative DNA damage in temperature-sensitive Pol III mutant requires ferrous ion

To investigate the involvement of Fe^{2+} in cell death and oxidative DNA damages in *dnaE486*(ts) mutant, I treated the MK7180*dnaE486*(ts) cultures with sub-lethal concentration of iron chelator 2,2'-bipyridine. This treatment led to a partial but significant suppression of mutation frequency in 42°C-treated *dnaE486*(ts) mutant (**Figure 3.26**), suggesting that Fe^{2+} is involved in the oxidative DNA damage. On the other hand, no significant difference was observed in the cell viability when comparing the bipyridine-treated and untreated cells (**Figure 3.27**). Taken together, the results indicated that the intracellular free Fe^{2+} is required for the oxidative DNA damage induction in temperature-sensitive Pol III mutant.

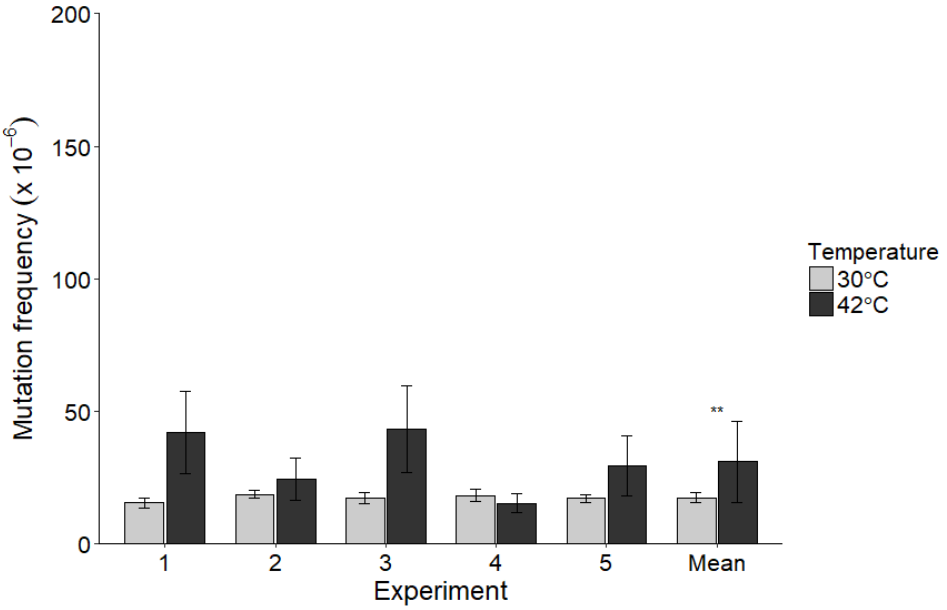

Figure 3.26 Bipyridine partially suppresses the oxidative DNA damages in Pol III mutant at non-permissive temperature. Bipyridine was added into MK7180*dnaE486*(ts) cultures 10 min before the cultures transfer to 42°C. Data points of each experiment represent the average of four replicas and the data point of mean represents the average of all five experiments. Error bars indicate standard deviation and the stars (**) indicate p-value <0.01.

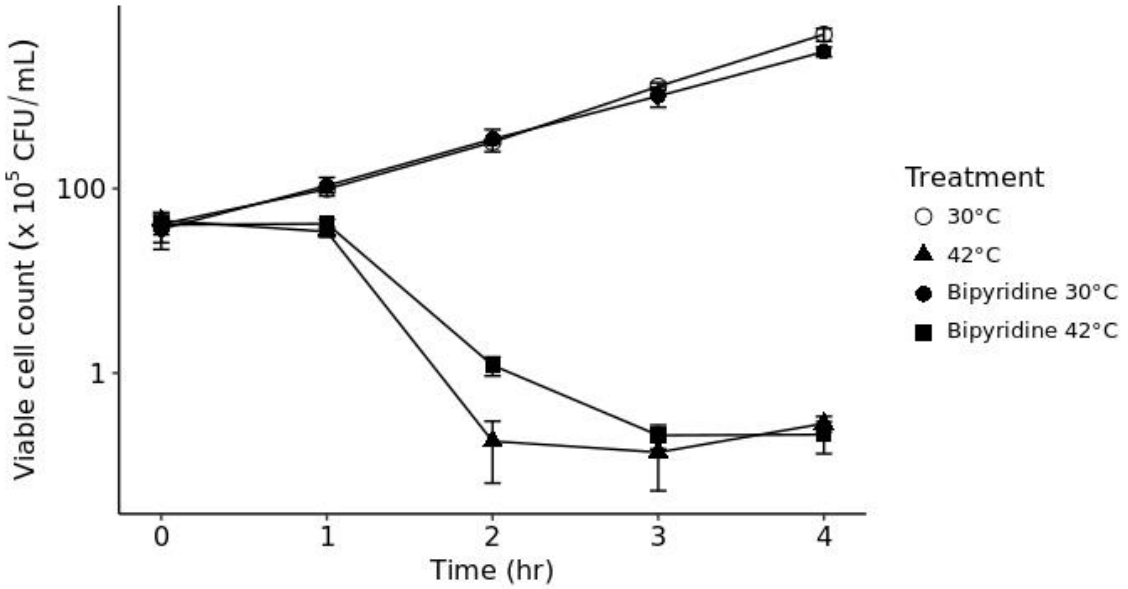

Figure 3.27 Survival curve of MK7180*dnaE486*(ts) grown at non-permissive temperature (42°C) in the presence (■) or absence (▲) of 0.2 mM bipyridine. Exponentially growing cultures were diluted to OD600 0.01 and treated with bipyridine for 10 min prior to transfer to 42°C. Each data point represents the average of three independent experiments, and the error bars represent the standard deviation of the independent measurements.

3. Cytochrome oxidase *bd*-I does not promote oxidative DNA damage in Pol III mutant at non-permissive temperature

Unlike the HU-treated cells, the absence of cytochrome oxidase *bd*-I in MK7180*dnaE486*(ts) did not show any reduction in oxidative DNA damage level at non-permissive temperature (**Figure 3.28**). Deletion of *cydAB* which encodes cytochrome oxidase *bd*-I further increased the oxidative DNA damage level in *dnaE486*(ts) mutant at 42°C. For the cell viability, MK7180Δ*cydABdnaE486*(ts) is slightly more sensitive to high temperature when compared to MK7180*dnaE486*(ts) (**Figure 3.29**).

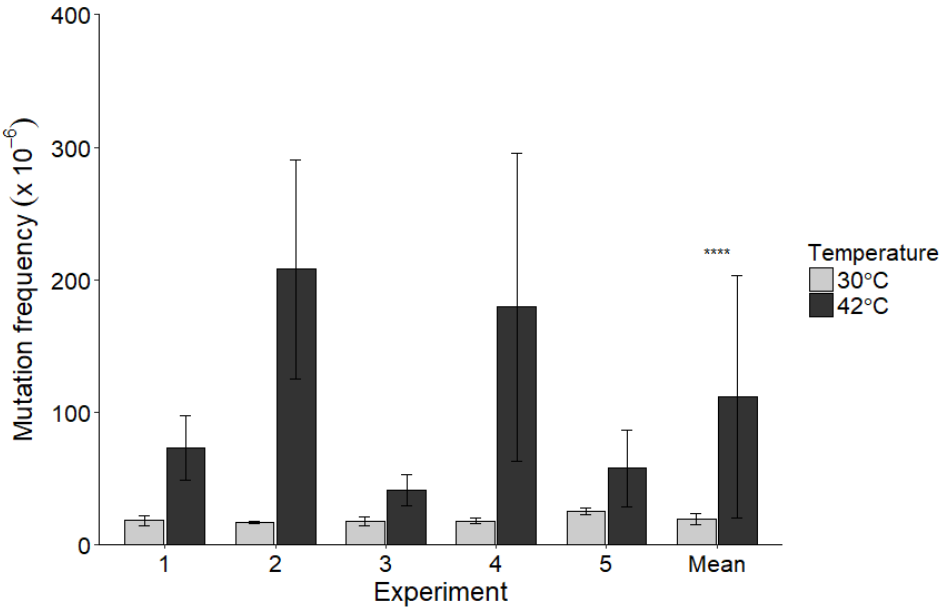

Figure 3.28 Deletion of *cydAB* further increase oxidative DNA damages in Pol III mutant at 42°C. MK7180Δ*cydABdnaE486*(ts) strain was used in this experiment. Data points of each experiment represent the average of four replicas and the data point of mean represents the average of all five experiments. Error bars indicate standard deviation and the stars (****) indicate p-value <0.0001.

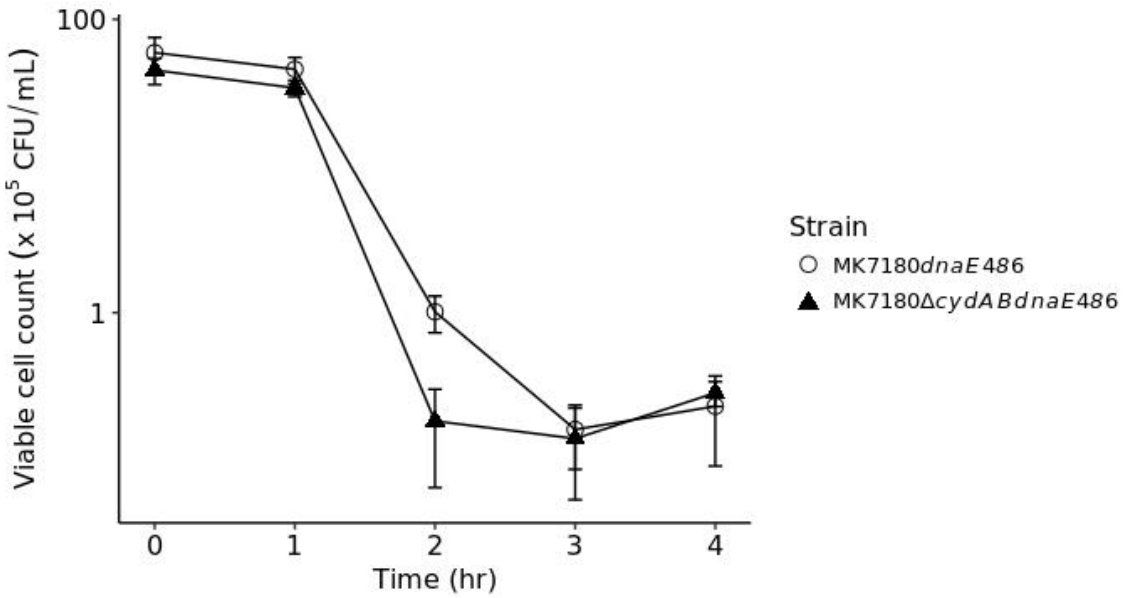

Figure 3.29 Deletion of *cydAB* accelerates the cell killing in Pol III mutant at non-permissive temperature. MK7180*dnaE486*(ts) (○) and MK7180Δ*cydABdnaE486*(ts) (▲) were incubated at 42°C. Each data point represents the average of three independent experiments, and the error bars represent the standard deviation of the independent measurements.

I also examined the effects of MazF toxin and Cpx membrane stress response system on the cell viability and mutation frequency of MK7180*dnaE468*(ts) strains at non-permissive temperature. Deletion of *mazF* did not significantly change the mutation frequency and cell viability of *dnaE*(ts) mutants at 42°C (**Figure 3.30 & 3.31**). In contrast, *cpxA*-deleted strain did show slight suppression in oxidative DNA damages level as compared to *cpxA*$^+$ strain. The mutation frequency of MK7180Δ*cpxAdnaE486*(ts) at 42°C was reduced ~1.6-fold compared to the *cpxA*$^+$ strain (**Figure 3.32**). However, the *cpxA*-deleted strain was more sensitive to high temperature (**Figure 3.33**). These results suggested that the Cpx membrane stress response system partially promotes the induction of oxidative DNA damages, but not cell killing, in *dnaE*(ts) mutant.

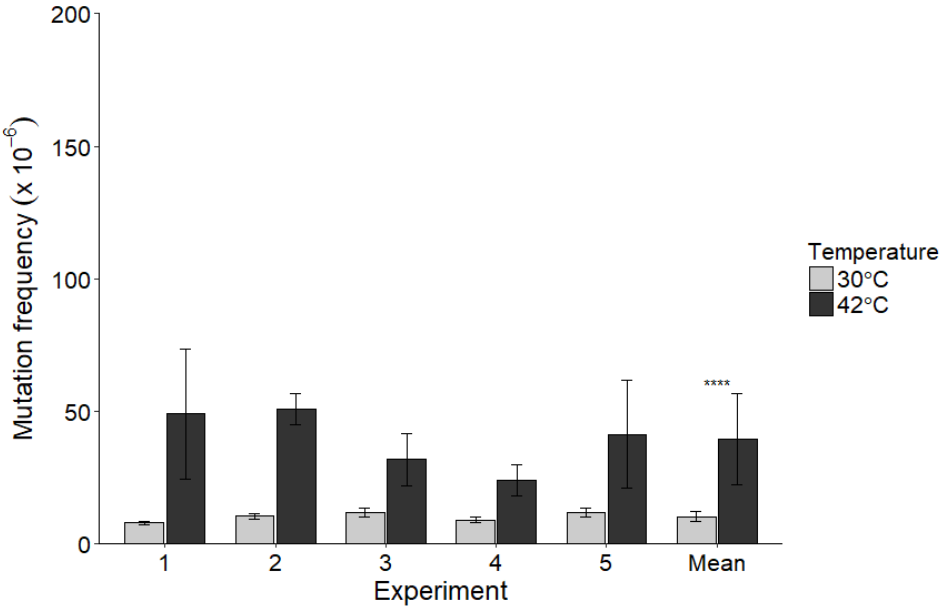

Figure 3.30 Deletion of *mazF* does not suppress oxidative DNA damages in Pol III mutant at 42°C. This experiment was performed by using MK7180Δ*mazFdnaE468*(ts) strain. Data points of each experiment represent the average of four replicas and the data point of mean represents the average of all five experiments. Error bars indicate standard deviation and the stars (****) indicate p-value <0.0001.

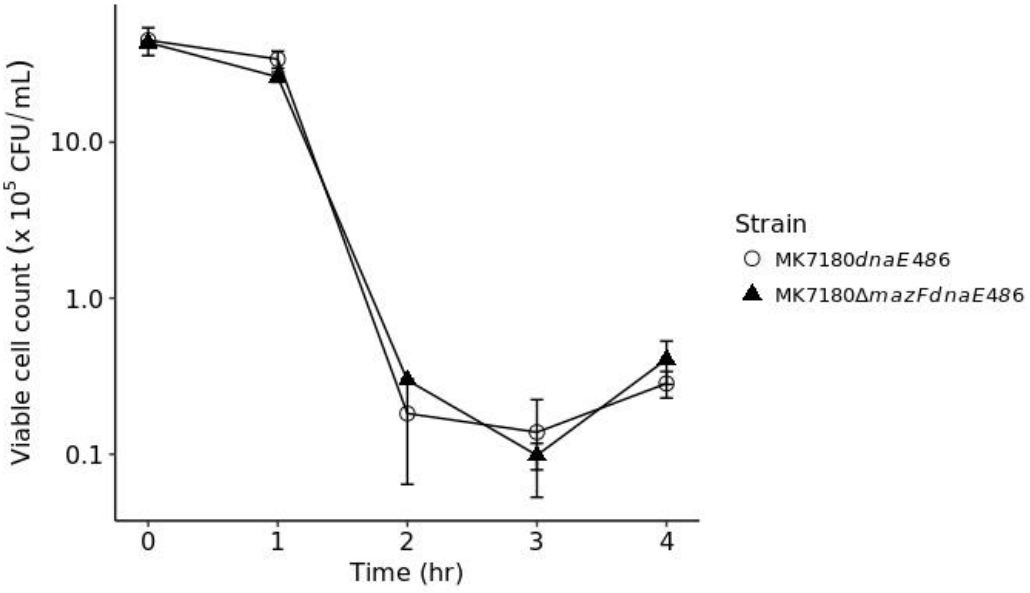

Figure 3.31 MazF toxin does not promote cell death in MK7180*dnaE486*(ts) strain at non-permissive temperature. MK7180*dnaE486*(ts) (○) and MK7180Δ*mazFdnaE486*(ts) (▲) were incubated at 42°C. Each data point represents the average of three independent experiments, and the error bars represent the standard deviation of the independent measurements.

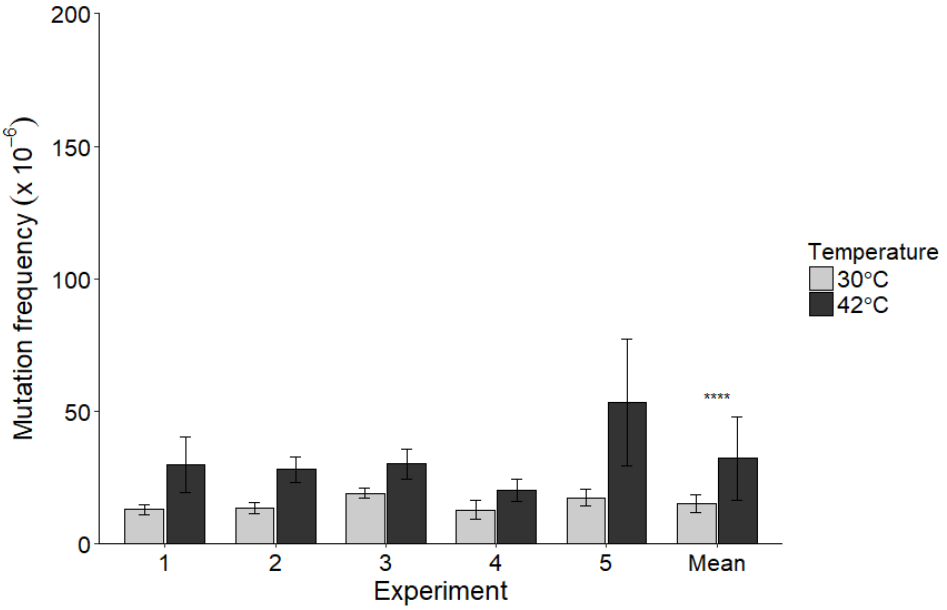

Figure 3.32 CpxAR system partially promotes oxidative DNA damages in Pol III mutant at 42°C. MK7180Δ*cpxAdnaE486*(ts) strain was used in this experiment. Data points of each experiment represent the average of four replicas and the data point of mean represents the average of all five experiments. Error bars indicate standard deviation and the stars (****) indicate p-value <0.0001.

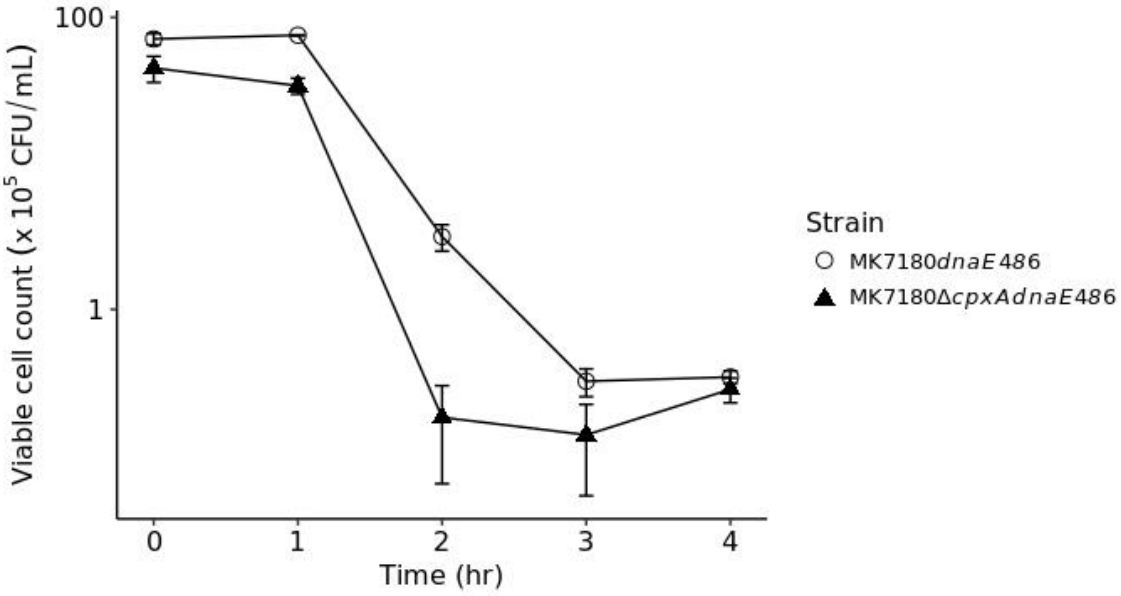

Figure 3.33 Deletion of *cpxA* in Pol III mutant accelerates cell death at non-permissive temperature. MK7180*dnaE486*(ts) (○) and MK7180Δ*cpxAdnaE486*(ts) (▲) were incubated at 42°C. Each data point represents the average of three independent experiments, and the error bars represent the standard deviation of the independent measurements.

Chapter 4 Discussions

1. HU induces oxidative DNA damage in *E. coli*

Hydroxyurea (HU) treatment has been reported to inhibit DNA replication progression via the targeted inhibition of class I ribonucleotide reductase (RNR), and leading to cell death when a large number of DNA double strand breaks accumulated. However, Collins and his colleagues proposed that cell death in *E. coli* under HU treatment is due to the hydroxyl radicals (OH•) production (Davies et al., 2009). Hydroxyl radical is deleterious to the cells because it can cause oxidative DNA damage. So far, there is no direct evidence to show that HU treatment can induce oxidative DNA damage in cells. In this study, I measured the cellular level of oxidative DNA damage using the mutation assay with strains carrying *mutM* and *mutY* double deletions (**Figure 3.1**). The result showed that the level of oxidative DNA damage increased about 4-fold when the cells were treated with 100 mM HU for 2 hours. Significant loss of cell viability was also observed after 2 hours of HU treatment (**Figure 3.3**). Furthermore, I found that both HU-induced oxidative DNA damage and cell death are completely suppressed by the addition of a potent hydroxyl radical scavenger, thiourea (**Figure 3.2 and 3.3**). Addition of thiourea, however, did not prevent HU-induced replication arrest because the viable cell number remains constant under such condition (**Figure 3.3**). My results indicated that HU treatment induces both oxidative DNA damage and cell death through the hydroxyl radical production. However, oxidative DNA damage might not be the primary cause of HU-induced cell death because it was recently found in our laboratory that normally growing cells are able to tolerate ~100-fold increase in oxidative DNA damage level without affecting the cell viability (Lan Anh, Doctoral thesis, 2017). Therefore, the ~ 4-fold increase in oxidative DNA damage level in HU-treated cells is unlikely the cause of cell death.

2. Involvement of cytochrome oxidase, but neither toxin-antitoxin nor membrane stress, in HU-induced oxidative DNA damage

Based on the observation that both oxidative DNA damage and cell death upon HU treatment can be significantly suppressed by hydroxyl radical scavenger, I hypothesized that HU-induced oxidative DNA damage might share the same molecular mechanism in HU-induced cell death proposed by Collins group (**Figure 1.6**). However, I obtained the results against the involvement of toxin-antitoxin and membrane stress systems in the oxidative DNA damage production and the HU-induced cell killing (**Figure 3.4-3.7**). The *mazF* mutant and *cpxA* mutant, which are defective in MazEF toxin-antitoxin system and Cpx membrane stress response system, respectively, did not show any suppression of the HU-induced oxidative DNA

damage (**Figure 3.5 and 3.7**). The slightly increased oxidative DNA damage level in *mazF* mutant suggested that MazEF toxin-antitoxin may play a protective role under HU treatment (**Figure 3.5**). Contrary to the Collins model, deletion of *mazF* or *cpxA* did not show any suppression of the cell killing by HU treatment (**Figure 3.4 and 3.6**). In the report by Davies *et al.*, MC4100 derivative strains carrying deletion of *mazEF* or *cpxA* showed an increased resistance to HU when the strains were spotted on LB agar plates containing different concentrations of HU ranging from 5 mM to 30 mM (Davies et al., 2009). However, by examining the viable cell count of the liquid cultures treated with 100 mM HU at different time points (**Figure 3.4 and 3.6**), I found that *mazF* or *cpxA* mutants did not prevent the HU-induced cell death. However, it should be noted that different strains of *E. coli* may differ in the HU sensitivity. Pentapeptide extracellular death factor (EDF) has been shown to activate the MazEF-mediated cell death under various kinds of stress conditions (Kolodkin-Gal et al., 2007). It has been also suggested that the commonly used *E. coli* strain MG1655 fails to produce EDF (Kolodkin-Gal & Engelberg-Kulka, 2008). Therefore, it is possible that the MG1655 derivatives may be more resistant to HU than the MC4100 derivatives. Even if this were the case, MazF toxin appeared to be dispensable for the HU-mediated cell killing.

Consistent with the data reported by Collins and his colleagues, I found that the HU-mediated cell death was completely suppressed by the deletion of *cydAB* genes (**Figure 3.8**). In addition, I also found that deletion of *cydAB* genes thoroughly suppressed the HU-induced oxidative DNA damage in *E. coli* cells (**Figure 3.9**). Cytochrome oxidase *bd* has been previously reported to display high catalase activity and suggested to protect cells against oxidative stress (Borisov et al., 2013). In agreement with this, the deletion of *cydAB* genes increased the oxidative DNA damage level to about 2-fold in untreated cells (**Figure 3.1 and 3.9**), indicating that cytochrome oxidase *bd*-I protects the *E. coli* cells from oxidative DNA damage under normal growth condition. Although higher oxidative DNA damage level was found in *cydAB* mutant when compared to the wild-type strain under normal condition, the addition of HU did not further increase the oxidative DNA damage in the *cydAB* mutant (**Figure 3.9**). These results suggested that cytochrome oxidase *bd*-I plays a protective role to reduce oxidative DNA damage in normally growing cells, but is required to induce oxidative DNA damage when the cells are treated with HU. My results also revealed that cytochrome oxidase *bo* and *bd*-II are not involved in HU-induced oxidative DNA damage (**Figure 3.10 and 3.11**). My data presented here establish an important role of the *cydAB*-encoded cytochrome oxidase *bd*-I in promoting HU-induced oxidative DNA damage as well as HU-induced cell death.

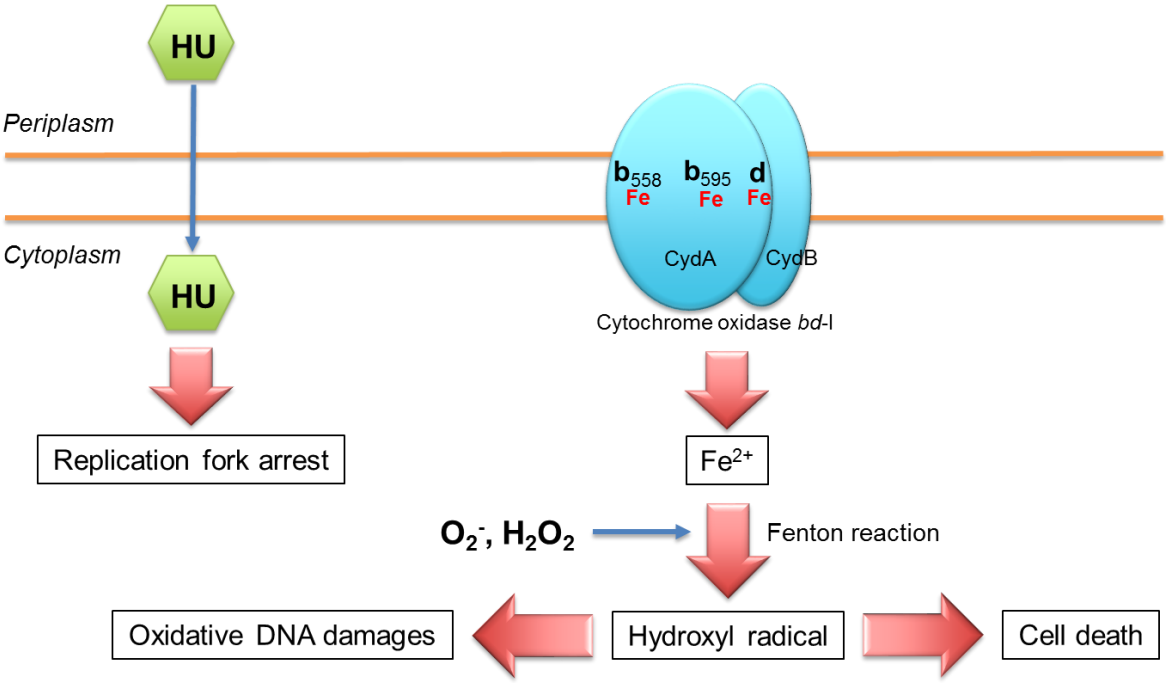

Figure 4.1 Summary figure of HU treatment in *E. coli*.

3. Cytochrome oxidase *bd*-I does not generate superoxide in HU-treated cells

The main source of intracellular ROS is the electron transport chain of the respiration system. Therefore, cytochrome oxidase *bd*-I could be the key enzyme that mediated the production of ROS upon HU treatment. Typically, the production of cytoplasmic superoxide is not the postulated action of cytochrome oxidases (Imlay, 2003). Collins and his colleagues proposed that HU treatment induces changes in the function of cytochrome oxidase *bd*-I so that leads to superoxide generation (Davies et al., 2009). Even though they observed a significant decrease in the superoxide level in a toxin-antitoxin mutant upon HU treatment, there is no direct evidence for the involvement of cytochrome oxidase *bd*-I in superoxide production in their study. By using a reporter assay system similar to one used by the Collins' group study, I found no difference in the superoxide level between HU-treated wild-type (*cydAB*$^{+}$) and *cydAB* mutant strain (**Figure 3.12 and 3.14**). These results clearly demonstrated that cytochrome oxidase *bd*-I is not responsible for superoxide production upon HU treatment. Since the superoxide dismutase (SOD) will quickly convert superoxide to hydrogen peroxide (H_2O_2) (Fridovich, 1983), measurement of H_2O_2 is an alternative approach to verify this observation. Indeed, I found that the cellular H_2O_2 level in the *cydAB* mutant was also similar to that in wild-type (*cydAB*$^{+}$) strain following HU treatment (**Figure 3.13 and 3.15**). This observation further supported that cytochrome oxidase *bd*-I is not involved in the generation of superoxide or H_2O_2 in the presence of HU.

4. Role of cytochrome oxidase *bd*-I in HU-treated cells

My results showed that cytochrome oxidase *bd*-I mediates the HU-induced hydroxyl radical production and is not responsible for the generation of superoxide or H_2O_2 upon HU treatment. Because hydroxyl radical formation is determined by intracellular H_2O_2 and free ferrous ion (Fe^{2+}) concentrations (**Figure 1.1**), I hypothesized that the intracellular free Fe^{2+} level might be affected by the cytochrome oxidase *bd*-I in the presence of HU. I examined this possibility by treating the cells with a potent iron chelator, 2,2-bipyridine. The addition of the iron chelator suppressed HU-induced oxidative DNA damage and cell death (**Figure 3.16 and 3.17**), implying that free Fe^{2+} plays an important role in both oxidative DNA damage and cell death in *E. coli* upon HU treatment. Even though the quantitation of intracellular free iron level in *E. coli* by electron paramagnetic resonance spectroscopy (EPR) was well established (Woodmansee & Imlay, 2002), difficulty in accessing the special spectrophotometer hindered the study, which is necessary to evaluate the effects of HU on the intracellular Fe^{2+} level.

Cytochrome oxidase *bd*-I is a heme-containing enzyme that mediates the reduction of oxygen to water by using ubiquinol as the reducing agent in *E. coli* cells (Dueweke & Gennis, 1990; Lorence et al., 1987). Therefore, I hypothesized that the heme from cytochrome oxidase *bd*-I might be the source of Fe^{2+} upon HU treatment. Previous studies showed that the substitution of Glu99 in CydA with Ala (E99A) results in reduced heme content in the cytochrome oxidase *bd*-I whereas substitution of Lys252 in CydA with Ala (K252A) results in a functionally defective mutant, maintaining heme content similar to the wildtype (Mogi, Endou, et al., 2006; Murali & Gennis, 2018). My results showed that *E. coli* cells expressing the E99A mutant significantly suppressed the HU-induced oxidative DNA damage and cell death (**Figure 3.18 and 3.20**). In contrast, no significant difference in oxidative DNA damage level and survival rate was observed between cells expressing wild-type cytochrome oxidase *bd*-I and cells expressing K252A oxidase mutant following HU treatment (**Figure 3.18 - 3.19 and 3.21**). These data indicated that the oxidase activity of cytochrome oxidase *bd*-I is not required for HU-induced oxidative DNA damage and cell death. Since cells expressing the E99A mutant showed a reduced oxidative DNA damage level similar to the *cydAB* mutant, it raised the question about the stability of the expressed E99A oxidase protein. However, due to the low expression level of cytochrome oxidase *bd*-I in the cells, I failed to observe any significant difference in the *cydAB* expression level between wild-type (*cydAB*$^+$) and *cydAB*$^-$ mutant strains as far as I analyzed total proteins from the strains by SDS polyacrylamide gel electrophoresis followed by CBB-staining (data not shown). Alternative experimental approaches such as membrane protein fractionation or expression of epitope tagged-cytochrome oxidase *bd*-I may be needed to examine the stability of E99A mutated oxidase.

The speculation that Fe^{2+} released from heme in cytochrome oxidase *bd*-I might be the cause of HU-induced oxidative DNA damage and cell death raised the question on whether the iron intake systems also facilitate the induction of oxidative DNA damage and cell death. To test this hypothesis, I disrupted a gene encoding the energy-transducing complex TonB, which provides energy to the iron uptake systems in *E. coli* cells (Moeck & Coulton, 1998; Noinaj et al., 2010). However, no significant reduction in HU-induced oxidative DNA damage was found in the *tonB* mutant (**Figure S1** in Supplementary), suggesting that extracellular Fe^{3+} are not involved in HU-induced oxidative DNA damage.

5. HU treatment *versus* temperature-sensitive Polymerase III mutant

My data described above clearly showed that HU induces oxidative DNA damage by producing hydroxyl radical and that cytochrome oxidase *bd*-I is most probably the key factor that promotes hydroxyl radical formation by affecting intracellular Fe^{2+}. Because HU is a DNA replication stress-inducing agent, it is possible that the molecular mechanism of HU-induced oxidative DNA damage could be generalized to other DNA replication stress conditions. To test this hypothesis, temperature-sensitive Pol III mutant (*dnaE486*) was used as an alternative source for DNA replication stress. *dnaE486* mutant causes replication arrest at non-permissive temperature (Wechsler & Gross, 1971). At non-permissive temperature, *dnaE486* mutant did exhibit an increase in hydroxyl radical level compared to the WT strain (Davies et al., 2009). In support to the previous observation, I found that the oxidative DNA damage was increased in *dnaE486* mutant when cells were incubated at non-permissive temperature, and the increased oxidative DNA damage was completely suppressed by the addition of hydroxyl radical scavenger, thiourea (**Figure 3.23 and 3.24**). However, the addition of thiourea did not prevent cell death of *dnaE486* mutant at non-permissive temperature (**Figure 3.22**). Altogether, my observations clearly demonstrated that the production of hydroxyl radical in *dnaE486* mutant only contributes to the oxidative DNA damage but not cell death. On the other hand, the increased level of oxidative DNA damage in *dnaE486* mutant was also suppressed by the addition of iron chelator bipyridine (**Figure 3.26**). This also indicates the involvement of Fe^{2+} in the induction of oxidative DNA damage in *dnaE486* mutant. Although the molecular mechanism of cell death induced by HU treatment and those induced by inactivation of Pol III are distinct, my study did reveal that both conditions could induce hydroxyl radical-mediated oxidative DNA damage in cells.

Since cytochrome oxidase *bd*-I was proved to be involved in the HU-induced oxidative DNA damage and cell death, I examined the possibility that cytochrome oxidase *bd*-I might play a role in the induction of oxidative DNA damage and cell death in the Pol III defective

mutant. However, I found that the disruption of cytochrome oxidase *bd*-I did not prevent cell death in the *dnaE486* mutant at non-permissive temperature (**Figure 3.29**). Furthermore, the absence of cytochrome oxidase *bd*-I in *dnaE486* mutant induced an even higher level of oxidative DNA damage compared to the *cydAB*$^{+}$ strain (**Figure 3.23 and 3.28**). These results indicated that cytochrome oxidase *bd*-I was not involved in the oxidative DNA damage induction and cell death in *dnaE486* mutant upon inactivation of Pol III. Taken together, my results revealed that the mechanisms of oxidative DNA damage induction are different between HU-treated cells and *dnaE486* mutant.

The mutation analysis with *cpxA* mutant revealed that the induction of oxidative DNA damage in *dnaE486* mutant at non-permissive temperature is affected by the Cpx membrane stress response system (**Figure 3.32**). This result further supports my previous observation whereby the molecular mechanism of oxidative DNA damage induction in HU-treated cells is different from those in the *dnaE486* mutant.

6. Possible molecular mechanism of HU-induced oxidative DNA damage

My work describes the previously unknown molecular mechanism by which HU treatment leads to oxidative DNA damage in *E. coli*. As shown in **Figure 4.2**, HU treatment induces both oxidative DNA damage and cell death in *E. coli* through cytochrome oxidase *bd*-I. This model is based on previous studies (Alvino et al., 2007; Davies et al., 2009; Poli et al., 2012), and includes speculations from the data obtained in this study. Once HU enters the cell and inhibits the class I ribonucleotide reductase (RNR) enzymes, it will cause rapid depletion of dNTP pool and arrest replication fork progression. Two-hours of HU exposure might cause damage to the cytochrome oxidase *bd*-I, which might lead to the release of heme. Since each heme contains a single iron atom, heme from cytochrome oxidase *bd*-I might affect the intracellular Fe^{2+} level. The change of intracellular Fe^{2+} level may accelerate the formation of DNA-damaging hydroxyl radical through Fenton reaction, causing oxidative DNA damages and cell death.

The mechanism by which HU affects cytochrome oxidase *bd*-I remains to be explored. Mutation assay with HU-resistant RNR mutant strain could be a good experimental approach to clarify which HU itself or the stalled fork due to the dNTP depletion, causes the cytochrome oxidase *bd*-I mediated HU-induced oxidative DNA damage. RNR enzyme is the known primary target for HU, but an S75T mutation in the R2 subunit of RNR enzyme has been shown to increase HU resistance of the cells (Sneeden & Loeb, 2004).

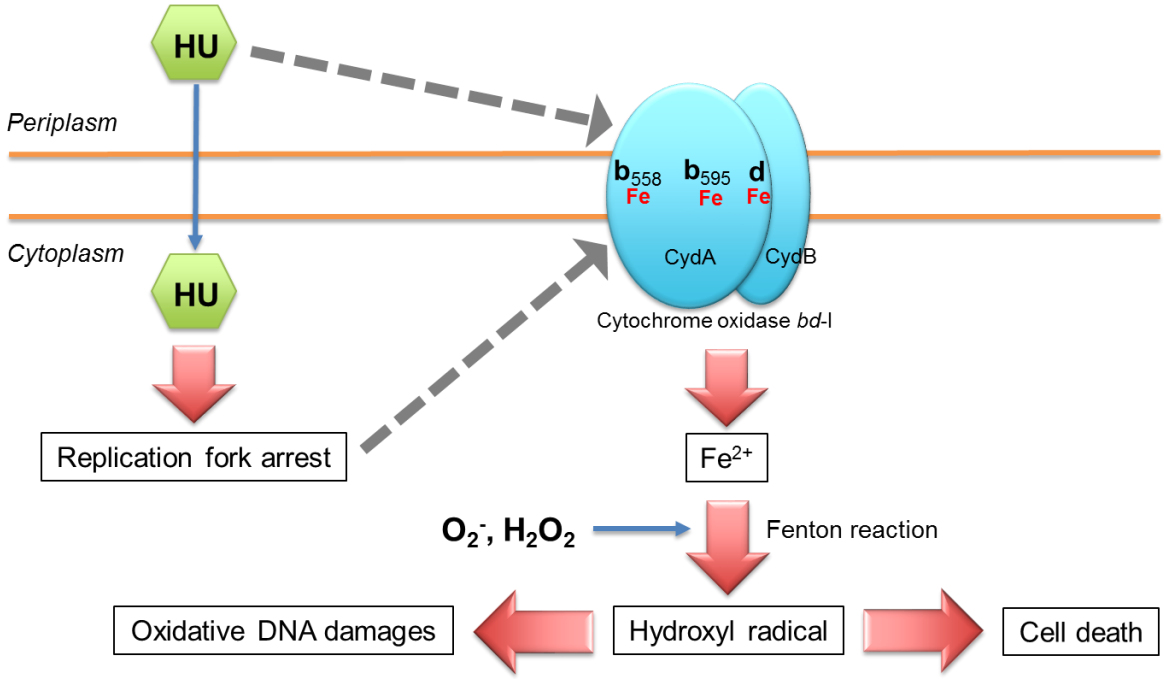

Figure 4.2 Proposed molecular mechanism for HU-induced oxidative DNA damage in *E. coli* cell.

Chapter 5 Conclusions

The *rpoB* mutation analyses with HU-treated Δ*mutM* Δ*mutY* double deletion mutant strains revealed that hydroxyurea (HU) does induce oxidative DNA damage and cell death. The induction of oxidative DNA damage and cell death is mediated by cytochrome oxidase *bd*-I. Even though cellular superoxide and H_2O_2 level are slightly increased upon HU treatment, the intracellular Fe^{2+} level seems to play a crucial role in HU-induced oxidative DNA damage. Since cells expressing mutated cytochrome oxidase *bd*-I that reduced in heme content showed a complete suppression on the HU-induced oxidative DNA damage, I speculated that heme from cytochrome oxidase *bd*-I could be the source of cellular Fe^{2+} upon HU treatment. However, further experiments are needed to confirm this speculation.

Mutation analyses in my study also demonstrated that temperature-sensitive Pol III mutant (*dnaE486*) at non-permissive temperature causes oxidative DNA damage through hydroxyl radical production, and the intracellular Fe^{2+} ion is an important factor for the oxidative DNA damage induction. However, the induction of oxidative DNA damage in *dnaE486* mutant upon Pol III inactivation is not mediated by the cytochrome oxidase *bd*-I.

In summary, both HU treatment and Pol III inactivation induce oxidative DNA damage in the cells through hydroxyl radical production. The intracellular Fe^{2+} level plays a crucial role in oxidative DNA damage induction. However, the molecular mechanism of oxidative DNA damage induction varies between HU-treated cells and Pol III mutant. Cytochrome oxidase *bd*-I is required for the induction of oxidative DNA damage in HU-treated cells, but not in the Pol III inactivation condition.

In conclusion, this study highlighted the molecular mechanism of HU-induced oxidative DNA damage, whereby the cytochrome oxidase *bd*-I and the intracellular Fe^{2+} level are the key players. This study also provided a new insight into the different mechanisms of oxidative DNA damage induction by HU-treated cells and Pol III mutants. This study expanded our current understanding of the effects and consequences of HU treatment, which could help to improve the present cancer treatment. Moving forward, it will be interesting to investigate how HU treatment affects the cytochrome oxidase *bd*-I in the cells.

Acknowledgements

First, I would like to express my deepest gratitude to my supervisor, Professor Dr. Hisaji Maki, for his advice, guidance and support throughout the project and giving me the opportunity to conduct my PhD research in his laboratory. With his guidance, his encouragement and his immense knowledge, I have gained a lot of scientific knowledge and learned to think logically in a scientific way.

Besides my supervisor, I would like to thanks my advisors, Professor Dr. Kaz Shiozaki and Professor Dr. Hiroshi Takagi, who have been giving me a lot of advice and comments throughout my PhD study.

I would like to express my appreciation to Associate Professor Dr. Masahiro Akiyama, Dr. Asako Furukohri and Dr. Satoko Maki for their help, suggestion and guidance.

I also would like to extend my thanks to my family for their support and encouragement. Thanks to my friends and lab mates who always giving me help and support.

Finally, I sincerely thank my dearest husband, Chin Lit Chein, for his love, care, support, encourage and understanding throughout my study in Japan. Without his support, I would not have been accomplish my thesis.

References

Abdul-Tehrani, H., Hudson, A. J., Chang, Y. S., Timms, A. R., Hawkins, C., Williams, J. M., … Andrews, S. C. (1999). Ferritin mutants of Escherichia coli are iron deficient and growth impaired, and fur mutants are iron deficient. *Journal of Bacteriology*, *181*(5), 1415–1428.

Aizenman, E., Engelberg-Kulka, H., & Glaser, G. (1996). An Escherichia coli chromosomal "addiction module" regulated by 3',5'-bispyrophosphate: a model for programmed bacterial cell death. *Proceedings of the National Academy of Sciences of the United States of America*, *93*(12), 6059–6063.

Alberts, B., Johnson, A., Lewis, J., Raff, M., Roberts, K., & Walter, P. (2002). The Initiation and Completion of DNA Replication in Chromosomes. In *Molecular Biology of the Cell* (4th edition). Garland Science.

Alhama, J., Ruiz-Laguna, J., Rodriguez-Ariza, A., Toribio, F., L6pez-Barea, J., & Pueyo, C. (1998). Formation of 8-oxoguanine in cellular DNA of Escherichia coli strains defective in different antioxidant defences. *Mutagenesis*, *13*(6), 589–594.

Alvino, G. M., Collingwood, D., Murphy, J. M., Delrow, J., Brewer, B. J., & Raghuraman, M. K. (2007). Replication in hydroxyurea: it's a matter of time. *Molecular and Cellular Biology*, *27*(18), 6396–6406.

Andrews, S. C., Robinson, A. K., & Rodríguez-Quiñones, F. (2003). Bacterial iron homeostasis. *FEMS Microbiology Reviews*, *27*(2–3), 215–237.

Barbui, T., Finazzi, M. C., & Finazzi, G. (2012). Front-line therapy in polycythemia vera and essential thrombocythemia. *Blood Reviews*, *26*(5), 205–211.

Barthelemy, J., Hanenberg, H., & Leffak, M. (2016). FANCJ is essential to maintain microsatellite structure genome-wide during replication stress. *Nucleic Acids Research*, *44*(14), 6803–6816.

Beck, H., Nähse-Kumpf, V., Larsen, M. S. Y., O'Hanlon, K. A., Patzke, S., Holmberg, C., … Sørensen, C. S. (2012). Cyclin-dependent kinase suppression by WEE1 kinase protects the genome through control of replication initiation and nucleotide consumption. *Molecular and Cellular Biology*, *32*(20), 4226–4236.

Belle, J. J., Casey, A., Courcelle, C. T., & Courcelle, J. (2007). Inactivation of the DnaB helicase leads to the collapse and degradation of the replication fork: a comparison to UV-induced arrest. *Journal of Bacteriology*, *189*(15), 5452–5462.

Benov, L. T., & Fridovich, I. (1994). Escherichia coli expresses a copper- and zinc-containing superoxide dismutase. *The Journal of Biological Chemistry*, *269*(41), 25310–25314.

Bester, A. C., Roniger, M., Oren, Y. S., Im, M. M., Sarni, D., Chaoat, M., … Kerem, B. (2011). Nucleotide deficiency promotes genomic instability in early stages of cancer development. *Cell*, *145*(3), 435–446.

Bierne, H., & Michel, B. (1994). When replication forks stop. *Molecular Microbiology*, *13*(1), 17–23.

Borisov, V. B., Forte, E., Davletshin, A., Mastronicola, D., Sarti, P., & Giuffrè, A. (2013). Cytochrome bd oxidase from Escherichia coli displays high catalase activity: An additional defense against oxidative stress. *FEBS Letters*, *587*(14), 2214–2218.

Bridge, G., Rashid, S., & Martin, S. A. (2014). DNA mismatch repair and oxidative DNA damage: implications for cancer biology and treatment. *Cancers*, *6*(3), 1597–1614.

Calhoun, L. N., & Kwon, Y. M. (2011). Structure, function and regulation of the DNA-binding protein Dps and its role in acid and oxidative stress resistance in Escherichia coli: a review. *Journal of Applied Microbiology*, *110*(2), 375–386.

Carr, A. M., & Lambert, S. (2013). Replication Stress-Induced Genome Instability: The Dark Side of Replication Maintenance by Homologous Recombination. *Journal of Molecular Biology*, *425*, 4733–4744.

Darzynkiewicz, Z., Halicka, H. D., Zhao, H., & Podhorecka, M. (2011). Cell synchronization by inhibitors of DNA replication induces replication stress and DNA damage response: analysis by flow cytometry. *Methods in Molecular Biology (Clifton, N.J.)*, *761*, 85–96.

Dasari, S., & Tchounwou, P. B. (2014). Cisplatin in cancer therapy: molecular mechanisms of action. *European Journal of Pharmacology*, *740*, 364–378.

Datsenko, K. A., & Wanner, B. L. (2000). One-step inactivation of chromosomal genes in Escherichia coli K-12 using PCR products. *Proceedings of the National Academy of Sciences*, *97*(12), 6640–6645.

Davies, B. W., Kohanski, M. A., Simmons, L. A., Winkler, J. A., Collins, J. J., & Walker, G. C. (2009). Hydroxyurea Induces Hydroxyl Radical-Mediated Cell Death in Escherichia coli. *Molecular Cell*, *36*(5), 845–860.

Dizdaroglu, M. (2012). Oxidatively induced DNA damage: Mechanisms, repair and disease. *Cancer Letters*, *327*(1–2), 26–47.

Dueweke, T. J., & Gennis, R. B. (1990). Epitopes of monoclonal antibodies which inhibit ubiquinol oxidase activity of Escherichia coli cytochrome d complex localize functional domain. *The Journal of Biological Chemistry*, *265*(8), 4273–4277.

Feng, W., Di Rienzi, S. C., Raghuraman, M. K., & Brewer, B. J. (2011). Replication stress-induced chromosome breakage is correlated with replication fork progression and is preceded by single-stranded DNA formation. *G3 (Bethesda, Md.)*, *1*(5), 327–335.

Flynn, R. L., & Zou, L. (2011). ATR: a master conductor of cellular responses to DNA replication stress. *Trends in Biochemical Sciences*, *36*(3), 133–140.

Fowler, R. G., & Schaaper, R. M. (1997). The role of the mutT gene of Escherichia coli in maintaining replication fidelity. *FEMS Microbiology Reviews*, *21*(1), 43–54.

Fowler, R. G., White, S. J., Koyama, C., Moore, S. C., Dunn, R. L., & Schaaper, R. M. (2003). Interactions among the Escherichia coli mutT, mutM, and mutY damage prevention pathways. *DNA Repair*, *2*(2), 159–173.

Fridovich, I. (1983). Superoxide Radical: An endogenous toxicant. *Annu Rev Pharmacol Toxicol*, *23*, 239–257.

Gaillard, H., García-Muse, T., & Aguilera, A. (2015). Replication stress and cancer. *Nature Reviews Cancer*, *15*(5), 276–289.

Godoy, V. G., Jarosz, D. F., Walker, F. L., Simmons, L. A., & Walker, G. C. (2006). Y-family DNA polymerases respond to DNA damage-independent inhibition of replication fork progression. *The EMBO Journal*, *25*(4), 868–879.

Guyer, M. S., Reed, R. R., Steitz, J. A., & Low, K. B. (1981). Identification of a sex-factor-affinity site in E. coli as gamma delta. *Cold Spring Harbor Symposia on Quantitative Biology*, *45 Pt 1*, 135–140.

Imlay, J. A. (2003). Pathways of Oxidative Damage. *Annual Review of Microbiology*, *57*(1), 395–418.

Imlay, J. A. (2008). Cellular Defenses against Superoxide and Hydrogen Peroxide. *Annual Review of Biochemistry*, *77*(1), 755–776.

Imlay, J. A., & Fridovich, I. (1991). Assay of metabolic superoxide production in Escherichia coli. *The Journal of Biological Chemistry*, *266*(11), 6957–6965.

Karas, V. O., Westerlaken, I., & Meyer, A. S. (2015). The DNA-Binding Protein from Starved Cells (Dps) Utilizes Dual Functions To Defend Cells against Multiple Stresses. *Journal of Bacteriology*, *197*(19), 3206–3215.

Keyer, K., & Imlay, J. A. (1996). Superoxide accelerates DNA damage by elevating free-iron levels. *Biochemistry*, *93*, 13635–13640.

Kohanski, M. A., Dwyer, D. J., Wierzbowski, J., Cottarel, G., & Collins, J. J. (2008). Mistranslation of Membrane Proteins and Two-Component System Activation Trigger Antibiotic-Mediated Cell Death. *Cell*, *135*(4), 679–690.

Kolberg, M., Strand, K. R., Graff, P., & Kristoffer Andersson, K. (2004). Structure, function, and mechanism of ribonucleotide reductases. *Biochimica et Biophysica Acta (BBA) - Proteins and Proteomics*, *1699*(1–2), 1–34.

Kolodkin-Gal, I., & Engelberg-Kulka, H. (2008). The extracellular death factor: physiological and genetic factors influencing its production and response in Escherichia coli. *Journal of Bacteriology*, *190*(9), 3169–3175.

Kolodkin-Gal, I., Hazan, R., Gaathon, A., Carmeli, S., & Engelberg-Kulka, H. (2007). A Linear Pentapeptide Is a Quorum-Sensing Factor Required for mazEF-Mediated Cell Death in Escherichia coli. *Science*, *318*(5850), 652–655.

Korshunov, S., & Imlay, J. A. (2006). Detection and quantification of superoxide formed within the periplasm of Escherichia coli. *Journal of Bacteriology*, *188*(17), 6326–6334.

Kreutzer, D. A., & Essigmann, J. M. (1998). Oxidized, deaminated cytosines are a source of C --> T transitions in vivo. *Proceedings of the National Academy of Sciences of the United States of America*, *95*(7), 3578–3582.

Kung, H. C., & Bolton, P. H. (1997). Structure of a duplex DNA containing a thymine glycol residue in solution. *The Journal of Biological Chemistry*, *272*(14), 9227–9236.

Lee, E. S., Heller, M. M., Kamangar, F., Park, K., Liao, W., & Koo, J. (2011). Hydroxyurea for the Treatment of Psoriasis including in HIV-infected Individuals: A Review. *Psoriasis Forum*, *17*(3), 180–187.

Li, X., Wright, P. M., & Lu, A. L. (2000). The C-terminal domain of MutY glycosylase determines the 7,8-dihydro-8-oxo-guanine specificity and is crucial for mutation avoidance. *The Journal of Biological Chemistry*, *275*(12), 8448–8455.

Liu, L. F., Desai, S. D., Li, T.-K., Mao, Y., Sun, M., & Sim, S.-P. (2006). Mechanism of Action of Camptothecin. *Annals of the New York Academy of Sciences*, *922*(1), 1–10.

Lorence, R. M., Carter, K., Green, G. N., & Gennis, R. B. (1987). Cytochrome b558 monitors the steady state redox state of the ubiquinone pool in the aerobic respiratory chain of Escherichia coli. *The Journal of Biological Chemistry*, *262*(22), 10532–10536.

Maki, H., & Sekiguchi, M. (1992). MutT protein specifically hydrolyses a potent mutagenic substrate for DNA synthesis. *Nature*, *355*(6357), 273–275.

Mazouzi, A., Velimezi, G., & Loizou, J. I. (2014). DNA replication stress: Causes, resolution and disease. *Experimental Cell Research*, *329*(1), 85–93.

Michaels, M. L., Cruz, C., Grollman, A. P., & Miller, J. H. (1992). Evidence that MutY and MutM combine to prevent mutations by an oxidatively damaged form of guanine in DNA. *Proceedings of the National Academy of Sciences of the United States of America*, *89*(15), 7022–7025.

Mironov, A., Seregina, T., Nagornykh, M., Luhachack, L. G., Korolkova, N., Lopes, L. E., … Nudler, E. (2017). Mechanism of H2S-mediated protection against oxidative stress in Escherichia coli. *Proceedings of the National Academy of Sciences of the United States of America*, *114*(23), 6022–6027.

Moeck, G. S., & Coulton, J. W. (1998). TonB-dependent iron acquisition: mechanisms of siderophore-mediated active transport. *Molecular Microbiology*, *28*(4), 675–681.

Mogi, T., Endou, S., Akimoto, S., Morimoto-Tadokoro, M., & Miyoshi, H. (2006). Glutamates 99 and 107 in Transmembrane Helix III of Subunit I of Cytochrome bd Are Critical for Binding of the Heme b 595 - d Binuclear Center and Enzyme Activity. *Biochemistry*, *45*(51), 15785–15792.

Mogi, T., Mizuochi-Asai, E., Endou, S., Akimoto, S., & Nakamura, H. (2006). Role of a putative third subunit YhcB on the assembly and function of cytochrome bd-type ubiquinol oxidase from Escherichia coli. *Biochimica et Biophysica Acta (BBA) - Bioenergetics*, *1757*(7), 860–864.

Montecucco, A., Zanetta, F., & Biamonti, G. (2015). Molecular mechanisms of etoposide. *EXCLI Journal*, *14*, 95–108.

Morafraile, E. C., Diffley, J. F. X., Tercero, J. A., & Segurado, M. (2015). Checkpoint-dependent RNR induction promotes fork restart after replicative stress. *Scientific Reports*, *5*(1), 7886.

Motamedi, M. R., Szigety, S. K., & Rosenberg, S. M. (1999). Double-strand-break repair recombination in Escherichia coli: physical evidence for a DNA replication mechanism in vivo. *Genes & Development*, *13*(21), 2889–2903.

Muñoz, S., & Méndez, J. (2017). DNA replication stress: from molecular mechanisms to human disease. *Chromosoma*, *126*(1), 1–15.

Murali, R., & Gennis, R. B. (2018). Functional importance of Glutamate-445 and Glutamate-99 in proton-coupled electron transfer during oxygen reduction by cytochrome bd from Escherichia coli. *Biochimica et Biophysica Acta (BBA) - Bioenergetics*, *1859*(8), 577–590.

Nakayashiki, T., & Mori, H. (2013). Genome-Wide Screening with Hydroxyurea Reveals a Link between Nonessential Ribosomal Proteins and Reactive Oxygen Species Production. *Journal of Bacteriology*, *195*(6), 1226–1235.

Neeley, W. L., & Essigmann, J. M. (2006). Mechanisms of Formation, Genotoxicity, and Mutation of Guanine Oxidation Products. *Chemical Research in Toxicology*, *19*(4), 491–505.

Noinaj, N., Guillier, M., Barnard, T. J., & Buchanan, S. K. (2010). TonB-Dependent Transporters: Regulation, Structure, and Function. *Annual Review of Microbiology*, *64*(1), 43–60.

Pogliano, J., Lynch, A. S., Belin, D., Lin, E. C., & Beckwith, J. (1997). Regulation of Escherichia coli cell envelope proteins involved in protein folding and degradation by the Cpx two-component system. *Genes & Development*, *11*(9), 1169–1182.

Poli, J., Tsaponina, O., Crabbé, L., Keszthelyi, A., Pantesco, V., Chabes, A., … Pasero, P. (2012). dNTP pools determine fork progression and origin usage under replication stress. *The EMBO Journal*, *31*(4), 883–894.

Raivio, T. L., & Silhavy, T. J. (1997). Transduction of envelope stress in Escherichia coli by the Cpx two-component system. *Journal of Bacteriology*, *179*(24), 7724–7733.

Sabatinos, S. A., & Forsburg, S. L. (2015). Managing Single-Stranded DNA during Replication Stress in Fission Yeast. *Biomolecules*, *5*(3), 2123–2139.

Seaver, L. C., & Imlay, J. A. (2001a). Alkyl Hydroperoxide Reductase Is the Primary Scavenger of Endogenous Hydrogen Peroxide in Escherichia coli. *Journal of Bacteriology*, *183*(24), 7173–7181.

Seaver, L. C., & Imlay, J. A. (2001b). Hydrogen peroxide fluxes and compartmentalization inside growing Escherichia coli. *Journal of Bacteriology*, *183*(24), 7182–7189.

Segal, J., John Strouse, M. J., Catherine Beach, M., Carlton Haywood, M., Catherine Witkop, M., Haeseong Park, M., … Sophie Lanzkron, M. (2008). *Hydroxyurea for the Treatment of Sickle Cell Disease*. *Agency for Healthcare Research and Quality*.

Sinha, R. P., & Häder, D.-P. (2002). UV-induced DNA damage and repair: a review. *Photochemical & Photobiological Sciences*, *1*(4), 225–236.

Sneeden, J. L., & Loeb, L. A. (2004). Mutations in the R2 subunit of ribonucleotide reductase that confer resistance to hydroxyurea. *The Journal of Biological Chemistry*, *279*(39), 40723–40728.

Soehnge, H., Ouhtit, A., & Ananthaswamy, H. N. (1997). Mechanisms of induction of skin cancer by uv radiation. *Frontiers in Bioscience*, *2*, 538–551.

Sørensen, C. S., & Syljuåsen, R. G. (2012). Safeguarding genome integrity: the checkpoint kinases ATR, CHK1 and WEE1 restrain CDK activity during normal DNA replication. *Nucleic Acids Research*, *40*(2), 477–486.

Strauss, B., Kelly, K., Dincman, T., Ekiert, D., Biesieda, T., & Song, R. (2004). Cell death in Escherichia coli dnaE(Ts) mutants incubated at a nonpermissive temperature is prevented by mutation in the cydA gene. *Journal of Bacteriology*, *186*(7), 2147–2155.

Tajiri, T., Maki, H., & Sekiguchi, M. (1995). Functional cooperation of MutT, MutM and MutY proteins in preventing mutations caused by spontaneous oxidation of guanine nucleotide in Escherichia coli. *Mutation Research/DNA Repair*, *336*(3), 257–267.

Touati, D., Jacques, M., Tardat, B., Bouchard, L., & Despied, S. (1995). Lethal oxidative damage and mutagenesis are generated by iron in delta fur mutants of Escherichia coli: protective role of superoxide dismutase. *Journal of Bacteriology*, *177*(9), 2305–2314.

Vandewiele, D., Fernández de Henestrosa, A. R., Timms, A. R., Bridges, B. A., & Woodgate, R. (2002). Sequence analysis and phenotypes of five temperature sensitive mutator alleles of dnaE, encoding modified α-catalytic subunits of Escherichia coli DNA polymerase III holoenzyme. *Mutation Research/Fundamental and Molecular Mechanisms of Mutagenesis*, *499*(1), 85–95.

Voineagu, I., Narayanan, V., Lobachev, K. S., & Mirkin, S. M. (2008). Replication stalling at unstable inverted repeats: Interplay between DNA hairpins and fork stabilizing proteins. *PNAS*, *105*(29), 9936–9941.

Walker, G. C. (1984). Mutagenesis and inducible responses to deoxyribonucleic acid damage in Escherichia coli. *Microbiological Reviews*, *48*(1), 60–93.

Wechsler, J. A., & Gross, J. D. (1971). Escherichia coli mutants temperature-sensitive for DNA synthesis. *MGG Molecular & General Genetics*, *113*(3), 273–284.

Weng, M., Zheng, Y., Jasti, V. P., Champeil, E., Tomasz, M., Wang, Y., … Tang, M. (2010). Repair of mitomycin C mono- and interstrand cross-linked DNA adducts by UvrABC: a new model. *Nucleic Acids Research*, *38*(20), 6976–6984.

Woodmansee, A. N., & Imlay, J. A. (2002). Quantitation of intracellular free iron by electron paramagnetic resonance spectroscopy. *Methods in Enzymology*, *349*, 3–9.

Zeman, M. K., & Cimprich, K. A. (2014). Causes and consequences of replication stress. *Nature Cell Biology*, *16*(1), 2–9.

Zhang, Y., Zhang, J., Hoeflich, K. P., Ikura, M., Qing, G., & Inouye, M. (2003). MazF Cleaves Cellular mRNAs Specifically at ACA to Block Protein Synthesis in Escherichia coli. *Molecular Cell*, *12*, 913–923.

Supplementary data

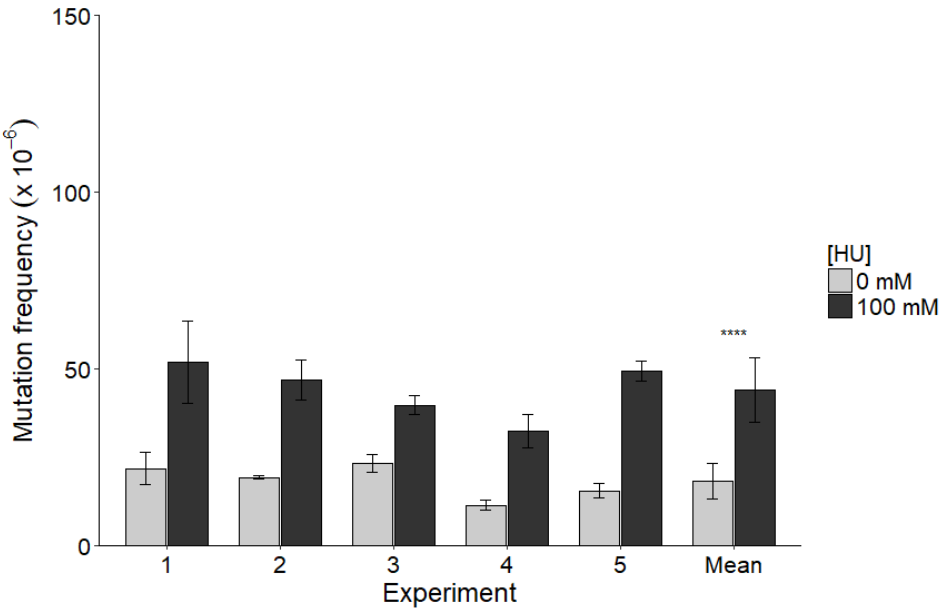

Figure S1 Disruption of TonB complex does not suppress oxidative DNA damage in HU-treated cells. This experiment was done by using MK7180Δ*tonB* strain. Data points of each experiment represent the average of four replicas and the data point of mean represents the average of all five experiments. Error bars indicate standard deviation and the stars (****) indicate p-value <0.0001.